Effects of KIF2A protein isoforms and *Kif2a* disease mutations on neuronal function

by

Cansu Akkaya

A Thesis Submitted to the
Graduate School of Sciences and Engineering
in Partial Fulfillment of the Requirements for
the Degree of

Master of Science

in
Molecular Biology and Genetics

Koc University

July 2015

Koc University

Graduate School of Sciences and Engineering

This is to certify that I have examined this copy of a master's thesis by

Cansu Akkaya

and have found that it is complete and satisfactory in all respects,
and that any and all revisions required by the final
examining committee have been made.

Committee Members:

_____

Gülayşe İnce-Dunn, Ph. D. (Advisor)

_____

Nurhan Özlü, Ph. D.

_____

Arzu Karabay Korkmaz, Prof. Dr.

Date: _____

ABSTRACT

RNA binding proteins (RNABP) are cytoplasmic and nuclear proteins that contain RNA recognition motifs (RRM). They bind to either single or double-stranded RNA and form ribonucleoprotein complexes. *Elavl2*, *Elavl3* and *Elavl4* are family members of a highly abundant nElavl (neuronal Embryonic Lethal Abnormal Vision-Like) RNABP. nElavl proteins regulate alternative splicing of numerous neuronal pre-mRNAs, by binding to specific intronic sequences. One of the major targets of nElavl is *Kinesin superfamily protein 2a (Kif2a)* pre-mRNA, encoded by a gene with roles in axonal branching, pruning and cortical development. In *Elavl3*/*4* double knockout mice *Kif2a* alternative splicing at exon 18 and consequently relative mRNA isoform abundance is altered. *Kif2a* gene encodes a motor protein, which in the cytoplasm acts as a microtubule depolymerase. KIF2A represses axon branching and elongation and *Kif2a* knock-out neurons display ectopic axonal branching and extra synapses at target regions. In humans *Kif2a* mutations cause malformations of cortical development. Currently, our understanding of the functional roles of different KIF2A isoforms is completely unknown. Our goal in this study was to identify differential functional roles for KIF2A protein isoforms by identifying their protein binding partners at a genome-wide level. Further we aimed to understand the cellular effects of disease causing *Kif2a* mutations. Our results demonstrated that the usage of exon18 in KIF2A protein affects the nature of its interacting protein partners; however it did not change KIF2A subcellular localization. Finally, humanized mutations in the motor domain of mouse *Kif2a* gene in primary cortical neurons resulted in abnormal KIF2A protein localization. Our results will shed light in understanding the molecular mechanisms by which the neuronal cytoskeleton is regulated and how it affects cortical development.

ÖZET

RNA'ya bağlanan proteinler (RNABP), RNA tanıyan motif içeren sitoplazmik ve çekirdek proteinleridir. Bu proteinler tek veya çift-sarmal RNA'ya bağlanıp ribonükleoprotein kompleksini oluştururlar. RNABP'lerden biri de nElavl (neuronal Embryonic Lethal and Abnormal Vision) familyasından *Elavl2, Elavl3* ve *Elavl4*'tür. nElavl proteinleri çok sayıdaki nöronal pre-mRNA'ların belirli intronik sekanslarına bağlanarak alternatif kırpılmasını düzenler. nElavl proteinlerinin başlıca hedefi olan *Kinesin süperfamilya protein 2a (Kif2a)* pre-mRNA'sı, aksonal dallanma, budanma ve korteks gelişiminde rolü olan gen tarafından kodlanır. *Elavl3/4* çift nakavt farelerde, ekson 18 alternatif kırpılması ve bununa ilişkin mRNA izoform miktarında değişiklik görülmüştür. *Kif2a* geni sitoplazmada mikrotübül depolimerazı olarak görev yapan motor proteinini kodlar. KIF2A akson dallanmasını ve uzamasını baskılar ve *kif2a* nakavt nöronlar ektopik akson dallanması ve hedef bölgelerde fazladan sinaps oluştururlar. İnsanlarda, *Kif2a* mutasyonları kusurlu korteks gelişimine neden olurlar. Farklı KIF2A izoformlarının fonksiyonel rolleri hakkında şuanda kesin bir bilgi yoktur. Bu çalışmada genom bazında KIF2A proteininin bağlandığı diğer protein partnerlerini tanımladık ve KIF2A izoformlarının farklı fonksiyonel rollerini araştırdık. Daha sonra, hastalık yaratan *Kif2a* mutasyonlarının hücresel etkilerini araştırdık. Sonuçlarımız, KIF2A proteininde ekson 18'in kullanılmasının bağlanılan protein partnerlerini etkilediği; fakat hücre içi yerleşimini etkilemediğini göstermektedir. Son olarak, primer nöron kültürlerinde, *Kif2a* geninin motor bölgesindeki mutasyonun anormal KIF2A protein yerleşimine neden olduğunu gösterdik. Sonuçlarımız, nöronal hucre iskeletini düzenleyen moleküler mekanizmaları ve bunların korteks gelişimini nasıl etkilediğini anlamamız için ışık tutacaktır.

ACKNOWLEDGEMENTS

I would like to express my sincere gratitude to my advisor Gülayşe İnce-Dunn, Ph.D for her understanding, wisdom, patience, enthusiasm and encouragements. Her guidance and persistent help opened my mind and gave me ability to look at my research in different ways. She gave me the right advice at the right time which was a great source of motivation for me in these two years. I have learned not only many valuable research techniques from her, but also how to handle a problem during experiments. I am extremely grateful that she accepted me in her lab for my master's and it has been a great pleasure and privilege to work with her. I would like thank Nurhan Özlü, Ph.D for helping me by sharing her knowledge and constructs and for critical reading on my thesis. I would also like to thank Cory Dunn, Ph.D and Elif Nur Fırat Karalar, Ph.D for sharing their knowledge, constructs and for their support. I would like to thank Arzu Karabay Korkmaz, Prof. Dr. for critical reading on my thesis.

I would like to acknowledge the financial support of the Scientific and Technological Research Council of Turkey (TÜBİTAK) and also Koç University throughout these two years.

I would like to thank my lab members Efil Bayam, Ph.D for her endless help and suggestions during my research, Semra Şahin, MSc and Gökhan Güner for all the tea breaks and good memories. Especially, I would like to thank my lab member and one of my dearest friends Gizem Güzelsoy for her support; we had lots of fun together both in and outside of the lab during these two years.

I would like to thank my two best friends Günce Bayram and Mehmet Gazaloğlu. They supported me throughout my graduate study and always cheered me up when I was down. They are the most amazing, thoughtful friends that a person could ever imagine and I know that they will always be there for me as my best friends through my entire life.

I would like to thank my cousin Nuray Kara Kuş, my roommates Hazal Aymandir and Bilgesu Erdoğan, and my friends Coşan Karadeniz, Burak Orhun Başer, Zeynep Cansu Üretmen, Onur Gültek, Deniz Kökçü, İlayda Gökçimen, Enes Uysal and Emre Sivrioğlu for their support and incredible memories.

I would also like to thank every single member of KOÇDANS family; especially Can Kara who stood by me and cheered me up every time I needed him, and my dance partner Murat Hoşgör for his support, great friendship and the useful advices he gave me when I had a problem.

The greatest thank goes to my family. They gave me lots of love at every step of my life and I know they will stand by me my whole life. I would like to thank my parents Nükhet Akkaya and Kemal Akkaya for their endless love, support and encouragements. I owe my success to them. I want to thank my aunt Nimet Gül for visiting me every time I got sick and for cooking me the most delicious foods; my brother-in-law Derya Saatçı for his support. Last but not least, I would like to thank my sister Pınar Akkaya Saatçı who I love the most in the world. She is the best sister in the world and is always there for me and supported me no matter what happened.

To my family....

TABLE OF CONTENTS

LIST OF TABLES

LIST OF FIGURES

NOMENCLATURE

3'UTR	3' untranslated region
APS	Ammonium persulfate
ATP	Adenosine triphosphate
BSA	Bovine Serum Albumin
BME	Basal Medium Eagle
bp	Basepair
cDNA	Complementary Deoxyribonucleic acid
DAPI	4',6-diamidino-2-phenylindole
DMEM	Dulbecco's Modified Eagle Medium
DMSO	Dimethyl sulfoxide
DNA	Deoxyribonucleic acid
dNTP	Deoxynucleotide
DTT	Dithiothreitol
EDTA	Ethylenediaminetetraacetic acid
nELAVL	Neuronal Embryonic Lethal and Abnormal Vision Like
FBS	Fetal Bovine Serum
GFP	Green Fluorescent Protein

HBSS Hank's Balanced Salt Solution

HEPES 4-(2-Hydroxyethly)piperazine-1-ethanesulfonic acid

HITS-CLIP High-throughput sequencing of RNA isolated by crosslinking immunoprecipitation

HRP Horseradish peroxidase

kDa Kilodalton

Kif2a Kinesin superfamily 2a

LB Luria Broth

MCD Malformations of Cortical Development

MEM Minimum Essential Media

mRNA Messenger Ribonucleic acid

MT Microtubule

NEM N-ethylmaleimide

PBS Phosphate Buffered Saline

PCR Polymerase Chain Reaction

PEI Polyethylenimine

PFA Paraformaldehyde

PIPKα Phosphatidylinositol-4-phosphate 5-kinase alpha

P/S	Penicillin/Streptomycin
Q-PCR	Quantitative Polymerase Chain Reaction
RNABP	Ribonucleic Acid Binding Protein
RIPA	Radioimmunoprecipitation Assay Buffer
RNA	Ribonucleic Acid
RRM	Ribonucleic Acid Recognition Motif
RT-PCR	Reverse Transcription Polymerase Chain Reaction
SDS-PAGE	Sodium Dodecyl Sulfate Polyacrylamide Gel Electrophoresis
TBS-T	Tris Buffered Saline-Tween
TEMED	Tetramethylethyleneamine

Chapter 1

INTRODUCTION

Expression of genes is controlled at transcriptional and post-transcriptional level [1], [2]. Post-transcriptionally differential polyadenylation, mRNA transport and stability, splicing, translation and degradation of transcripts affects gene expression [1], [3]. These post-transcriptional regulatory mechanisms have the advantage of making a dynamic and rapid response when the environmental conditions change. This biological view is especially relevant in highly specialized cells like neurons. In neurons, the protein content in specific subcellular compartments like axons, dendrites and growth cone has to be controlled dynamically and regulated in embryogenesis for appropriate neuronal differentiation and neuronal plasticity [1], [4].

During post-transcriptional regulation of gene expression, RNA-binding proteins (RNABP) are active players that behave synergistically or competitively to decide the fate of the transcript endowed with multiple cis-acting motifs [1], [5]. RNABPs are found in both nucleus and cytoplasm and they bind to either single or double-stranded RNA on their RNA recognition motifs (RRMs) to form ribonucleoprotein complexes. Various RNABPs play roles in neural development and maintenance in the brain. Among these ELAV (Embryonic Lethal Abnormal Vision-Like) proteins are highly conserved RNABP phylogenetically and display neuronal-restricted expression pattern [1], [6]. *Elavl2*, *Elavl3* and *Elavl4* are family members of a highly abundant neuronal Elavl (nElavl) RNABPs which were discovered as autoantigens in multisystem neurologic disorder termed as

paraneoplastic syndrome [1], [7]. These nELavl proteins bind to the specific intronic regions to regulate the alternative splicing of multiple pre-mRNAs [2].

One of the targets of nElavl is *Kinesin superfamily protein 2a (Kif2a)* pre-mRNA which has roles in axonal pruning, branching and development of cortex [8], [9], [10]. Deletion of *Elval3/4* affect the isoform abundance by affecting the *Kif2a* pre-mRNA alternative splicing [8]. Ince-Dunn *et al.* showed that nElavl proteins bind directly to the GU-rich intronic sequence flanking the alternative exon 18 [8].

Kinesin superfamily proteins (KIFs) are microtubule-dependent motor proteins that function in intracellular transport and division of cells. *Kif2a* is a member of the kinesin superfamily and serves as microtubule depolymerizers which is critical in cellular morphogenesis and mammalian development[11]. Homma *et al.* showed that *Kif2a-/-* mice have multiple brain abnormalities, migratory defects as well as abnormal axonal collateral branching [10]. Moreover, KIF2A has a role in microtubule depolymerization by binding monomers of microtubules (α and β tubulins) and this process causes axonal pruning in neurons [12]. I found that in the developing cortex KIF2A has three different isoforms; KIF2A.1 which contains complete exon 5 and exon 18, KIF2A.2 which contains complete exon 5 but not exon 18 and KIF2A.3 which contains parts of exon 5 and exon 18. Currently, our understanding of the functional roles of these different KIF2A isoforms is completely unknown. Recent reports demonstrated that missense mutations in the motor domain of *Kif2a* cause abnormal cortical development in humans [9]. Two mutations were identified, change in the nucleotide from guanine to adenine caused a change in the amino acid from serine to asparagine (KIF2A_S317N) and change in the nucleotide from cytosine to guanine caused a change in the amino acid from histidine to aspartic acid (KIF2A_H321D) [9]

KIF2A isoforms and mutants may have differential protein binding partners. In order to identify these differential protein binding partners, the BioID method is performed which is a unique method that is used to screen protein interactions that are physiologically relevant in living cells [13]. This technique is based on expressing biotin ligase fusion of KIF2A in cells, followed by streptavidin bead isolation of biotinylated proteins and mass spectrometric characterization. According to results from BioID method, analysis of the differential interacting protein partners of KIF2A isoforms and mutants will be done and their roles on cortical development will further be investigated.

In Chapter 2, there is a review of current literature about regulation of nElavl protein on *Kif2a* pre-mRNA splicing and functional roles of KIF2A protein, its isoforms and mutants. In Chapter 3, the materials and methods that used in this study are explained. The results of my project are presented in Chapter 4 and finally, the importance and implications for neuronal differentiation and cortex development are explained in Chapter 5.

Chapter 2

LITERATURE REVIEW

2.1 Overview

During development of the nervous system, the ordered production and differentiation of cell types are controlled tightly by gene expression mechanisms. Spatial and temporal gene expressions in neurons are regulated by both transcriptional and post-transcriptional mechanisms. RNA-binding proteins are on the center of post-transcriptional regulation and in eukaryotes, they have roles in regulating the abundance, form and stability of RNA which can be coding or non-coding [14]. The mammalian ELAVL/Hu (Embryonic Lethal and Abnormal Vision-Like) family which contains four RNABPs (ELAVL1, ELAVL2, ELAVL3 and ELAVL4) has roles in many biological processes [15]. nElavl (neuronal Elavl) proteins which are composed of ELAVL2, ELAVL3 and ELAVL4 are specifically expressed in neurons and bind preferably to GU-rich sequences of target RNAs both *in vitro* and *in vivo* regulating the alternative splicing in a position dependent manner. One of the target mRNAs that nELAVL regulates is *Kif2a* (Kinesin superfamily 2a) [8]. *Kif2a* encodes a protein which is a crucial executor of microtubule (MT) depolymerization and axonal breakdown during axonal pruning [12].

Neurons are highly polarized type of cells which depend on the microtubule cytoskeleton in development and physiology [16], [17]. Since KIF2A has a role in MT depolymerization, it affects the activity of growth cones and axons in neurons [10]. So far two alternative mRNA isoforms of *Kif2a* have been reported [18]. KIF2A has a motor

domain in the middle of the protein. Its role in MT depolymerization is ATP-dependent. So far a direct involvement in MT-based motility has not been shown [9], [10]. Missense mutations of Ser317 and His321 residues have been associated with cortical malformations [9]. These residues are conserved and located around the nucleotide binding pocket suggesting impaired binding and/or ATP hydrolysis [9].

2.2 RNA binding proteins: ELAVL family

The regulation of post-transcriptional gene expression evolved as a dominant activity throughout the evolution of eukaryotes. It increases both complexity of organisms and proteome diversity in higher organisms. These post-transcriptional regulations such as RNA editing, alternative splicing and regulation of 3' UTR are very common in the nervous system. Interactions of RNA binding proteins (RNABPs) with *cis*-acting elements located on RNA regulate tissue-specific alternative splicing and 3'UTR regulation. These kinds of interactions either inhibit or increase the recruitment of the regulatory machinery [8], [19].

In the nervous system, even though very large fractions of RNABPs are expressed, their RNA targets and these targets' roles are mostly unknown [8], [14]. One of the highly abundant RNABP family is ELAV/Hu (Embryonic Lethal and Abnormal Vision) [8]. *Elavl* (Elav-like) genes are highly conserved and share important homology with the *Drosophila ELAV* gene. The human orthologous of ELAV proteins were discovered as autoantigens of an autoimmune disorder of the nervous system associated with small cell lung carcinoma called paraneoplastic syndrome. In this disorder, ELAVL antigens are ectopically produced by lung cancer cells. An antibody-mediated immune response against the ELAVL antigens crosses the blood brain barrier attacking the neurons [1], [7], [20].

This highly conserved ELAVL family consists of four family members; *Elavl1 (HuA/HuR), Elavl2 (HuB), Elavl3 (HuC)* and *Elavl4 (HuD).* These four mammalian ELAVL have molecular weight about 40 kDa and each of the *Elavl* contains two RNA recognition motifs (RRM1 and RRM2) at their N-terminus and one RRM (RRM3) at their C-terminus which is separated by one flexible hinge region. The RRM1 and RRM2 have role in recognizing and binding the target RNA sequences and RRM3 plays role in binding to poly(A) tail and enhances the stability of RNA-protein complex [8], [19], [1], [21], [22]. *Elavl1* is expressed in a wide range of non-neuronal tissues in mammals and plays role in positive/negative regulation of mRNA stability, enhancement or repression of translation, splicing, polyadenylation, DNA damage response, negative regulation of apoptosis, carcinogenesis and inflammation. *Elavl2, Elavl3* and *Elavl4* are expressed specifically in the nervous system so they are referred to collectively as *nElavl* (neuronal Elavl). These nELAVL have roles in positive regulation of mRNA stability, splicing, translation enhancement, polyadenylation, neuronal differentiation, neuronal maintenance, learning and memory [8], [1], [15], [6]. Akamatsu *et al.* reported that knocking out the *Elavl4* gene causes brief delay of cranial nerve development in the embryonic day 10 (E10) mice, failure in reproduction and defects in the motor ability in adult mice [23]. Moreover, Ince-Dunn *et al.* studied the *Elavl3* null mice which have defects in cortical and cerebellar development [8].

2.3 Regulation of nELAVL proteins on *Kif2a* pre-mRNA splicing

Ince-Dunn *et al.* used high-throughput sequencing of RNA isolated by crosslinking immunoprecipitation (HITS-CLIP) method to find binding sites of nElavl and found that nElavl preferably binds to GU-rich sequences at exon-intron junctions and secondly to AU-rich sequences[8]. nElavl proteins regulate the alternative splicing of several pre-mRNAs by binding to these intronic sequences in a position dependent manner and they either repress or enhance the inclusion of an alternative exon. Moreover, nElavl proteins bind to 3'UTR for regulating mRNA levels [8]. For alternative splicing role of nElavl, Ince-Dunn *et al.* verified thirty-seven Elavl3/4 dependent alternative exons by RT-PCR [8]. *Kinesin superfamily protein 2a (Kif2a)* is one of the top target pre-mRNAs which has a role in axonal pruning by depolymerizing the microtubules and development of the cortex [8], [10], [12]. nElavl binds to U-rich intronic sequences flanking the alternative exon 18 (Figure 2.1A). Deletion of *Elavl3/4* has an effect on *Kif2a* pre-mRNA alternative splicing by enhancing the formation of isoform 1 (KIF2A.1) that contains the alternative exon 18 and repressing the formation of isoform 2 (KIF2A.2) that lacks alternative exon 18 (Figure 2.1B).

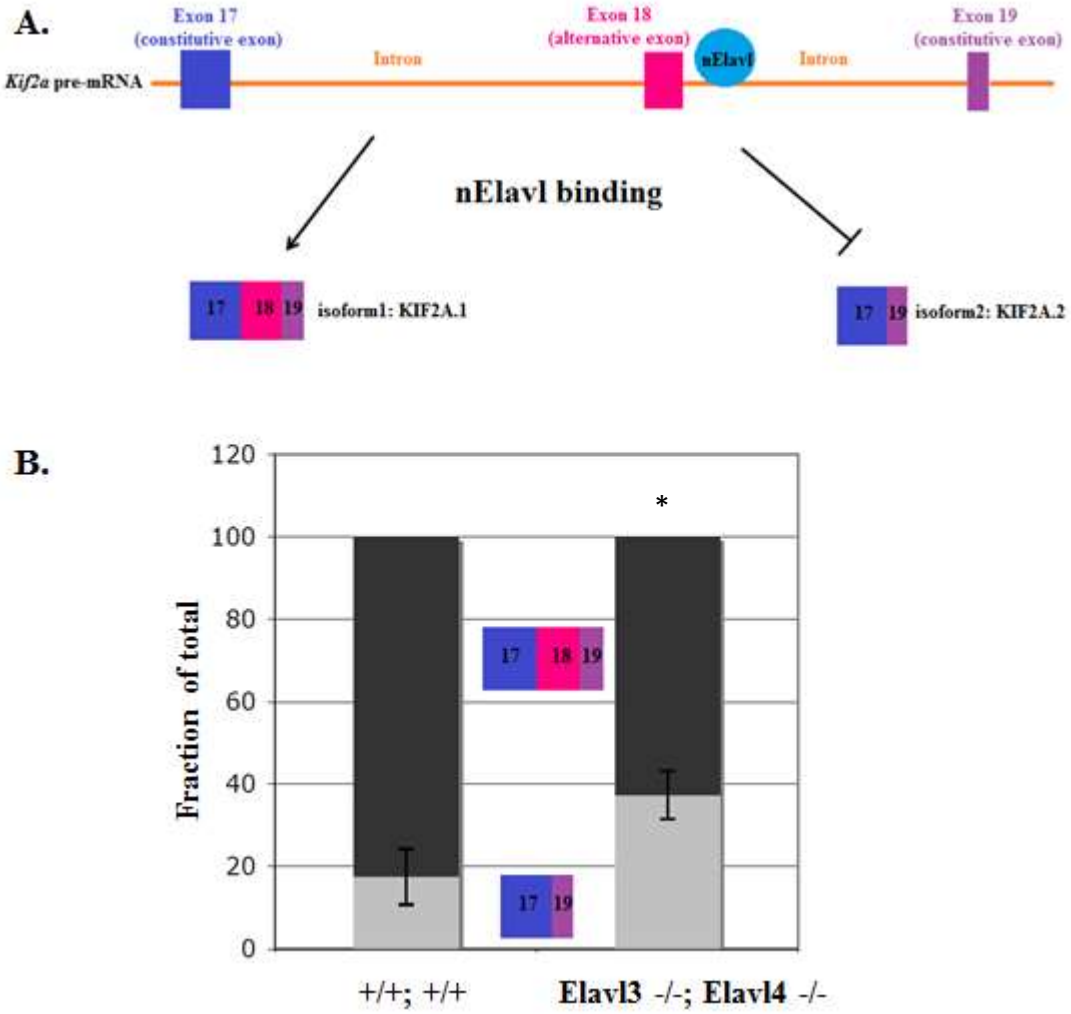

Figure 2.1: nELAVL proteins have roles in the neuronal alternative splicing. **A.** nELAVL binds directly to intronic elements in the intronic regions flanking the *Kif2a* alternative exon 18. **B.** Deletion of *Elavl3/4* affects the KIF2A isoform abundance [8].

2.4 Kinesin Superfamily and their associations with microtubules (MTs)

Molecular motor proteins generate cellular forces and drive numerous forms of intracellular movement [24], [25]. Kinesins are one of the main molecular motor proteins that are identified initially as molecular motor proteins for axonal transport [11], [26], [27], [28]. Most of the kinesins are plus-end directed microtubule (MT) motor proteins that are found in the cytoplasm during interphase [24]. More than 45 KIF proteins are found in mammals [11], [29], [30]. Almost half of the KIFs are expressed in neurons and have roles in the transport of several membranous organelles. Some KIFs which are expressed ubiquitously have roles in intracellular transport [11], [27], [28]. Among KIFs, M-kinesins are unique because they have a motor domain in the middle of the primary protein sequence [10]. Recent studies have shown that, KIFs are regulators of microtubule dynamics. Moreover, members of Kinesin-8 and Kinesin-13 families depolymerize microtubules. On the other hand, family members of Kinesin-4 and Kinesin-11 are microtubule stabilizers. Therefore, these atypical KIF proteins play important roles in cellular morphogenesis [11]. Recent studies have demonstrated that when these KIFs are deleted in knock-out mice, cellular morphology is affected in a critical manner [7], [10], [11], [31], [32]. Moreover, mutations in *Kif2a* and *Kif21a* have been shown to cause neuronal disorders in humans [9], [33].

2.5 Kinesin Superfamily Protein 2A (KIF2A)

Kinesin-13 family is composed of three members; Kif2a, Kif2b and MCAK/Kif2c [34], [35]. Subcellularly Kif2a is localized to spindle MTs and poles in mitotic cells and to growth cones and axons in neurons [34], [36], [37], [18]. KIF proteins -except KIF2A- contain their motor domains at either their N-terminus or C-terminus. However, KIF2A contains its motor domain in the central part [11], [18], [38]. It depolymerizes MTs in an ATP-dependent manner at both plus and minus ends of MTs [11], [39]. Homma *et al.* showed that KIF2A is not essential for cell division by creating *kif2a* knock-out mice which developed into neonates [10], [11]. On the other hand, *kif2a* knock-out mice died after birth due to neuronal abnormalities. These mice had defects in neuron morphology such as abnormal lateral axonal extensions as well as abnormal MT elongation in growth cone. Therefore, Homma *et al.* concluded that KIF2A controls the MT dynamics both in growth cone and axonal length [10], [11]. Moreover, mutations in *Kif2a* causes malformations in cortical development in humans [9].

Noda *et al.* suggested that KIF2A is regulated by binding to phosphatidylinositol-4-phosphate 5-kinase alpha (PIPKα) directly [11], [38]. They showed this regulation by knocking down PIPKα in cells and observing an increase in the axonal branches. MTs became more stable and extended to the plasma membrane. This morphology was observed also in both KIF2A knock-out and knock-down neurons which suggests that PIPKα and KIF2A work together *in vivo* [11], [38].

2.6 Isoforms of KIF2A

Ince-Dunn *et al.* reported that nElavl binds to *Kif2a* pre-mRNA [8]. This binding enhances the inclusion of alternative exon 18 which is one isoform (KIF2A.1) and represses the exclusion of alternative exon 18 which is the second isoform (KIF2A.2). In recent years our lab identified third isoform which contains the alternative exon 18 and a truncated exon 5 (KIF2A.3). Thus, there are three different KIF2A isoforms in neurons (Figure 2.2) and functional roles are unknown. All three isoforms contain motor domain in the middle where the ATP binding sites are present. They also contain MT binding site on their motor domain where MTs binds to and this binding causes depolymerization of the MTs. Moreover, they all contain dimerization domain and KIF2A is functional in a dimer form.

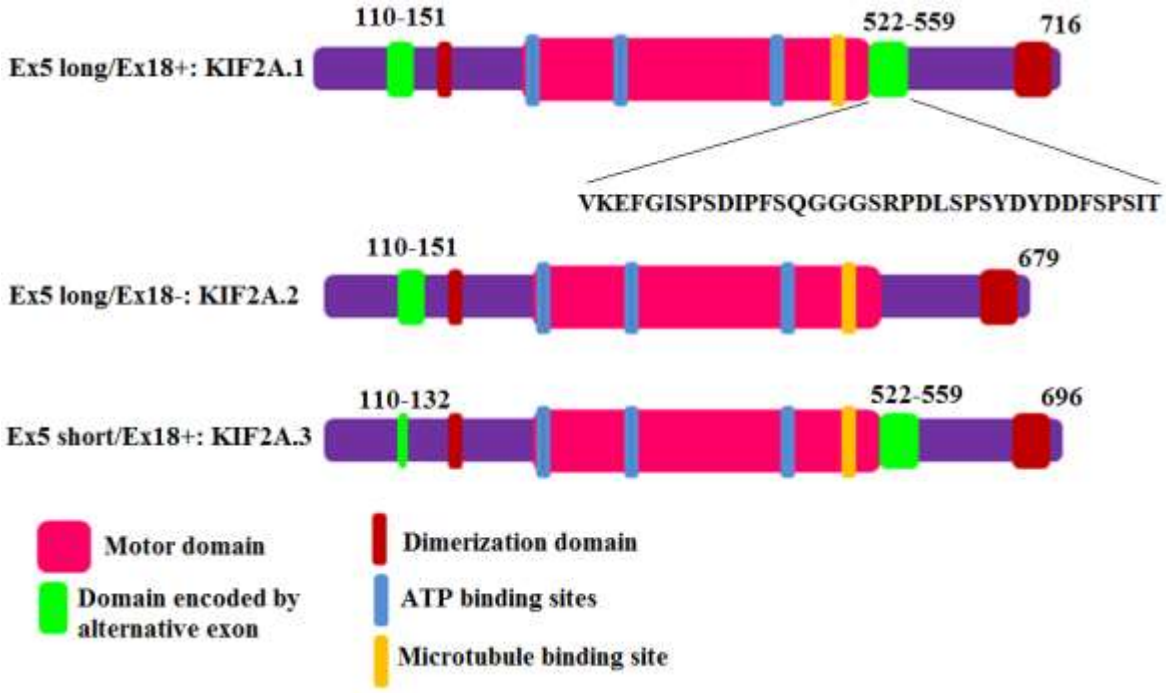

Figure 2.2: There are 3 different KIF2A isoform shown as KIF2A.1, KIF2A.2 and KIF2A.3.

2.7 Mutations on *Kif2a* cause malformations of cortical development

The mammalian brain has a very complex structure and it needs coordinated processes of migration, layering and timing of proliferation. Moreover, it requires differentiation of distinct neuronal population [9], [40], [41]. When these developmental processes are disrupted cortical development disorders such as pachygyria, microcephaly, polymicrogyria and lissencephaly is observed [9], [42]. Several mutations in genes which disrupt cerebral cortex development hence, cause cortical malformations were identified. These genes are collectively called as malformations of cortical development (MCD)-related genes and one of them is *kif2a* [9].

Poirier *et al.* identified two different heterozygous missense mutations that have dominant-negative effects and cause malformations on cortical development in humans [9]. First missense mutation was observed in a female patient who had neonatal onset seizures, posterior predominant pachygyria, frontal band heteropia and severe congenital microcephaly with thick cortex and thin corpus callosum. This patient had a genetic mutation on the ATP binding site of kinesin motor domain on *Kif2a* and this mutation occurred because of a change in the nucleotide from guanine to adenine causing a change in the amino acid sequence from serine to asparagine (KIF2A_S317N), (Figure 2.3). Second missense mutation was identified in a girl who had posterior predominant pachygyria and congenital microcephaly with subcortical band heterotopias and a thin corpus callosum. This patient's mutation was just after the ATP binding site, but still on the kinesin motor domain on *kif2a.* This missense mutation was a change in a single nucleotide from cytosine to guanine which caused a change in the amino acid sequence from histidine to aspartic acid (KIF2A_H321D), (Figure 2.3) [9].

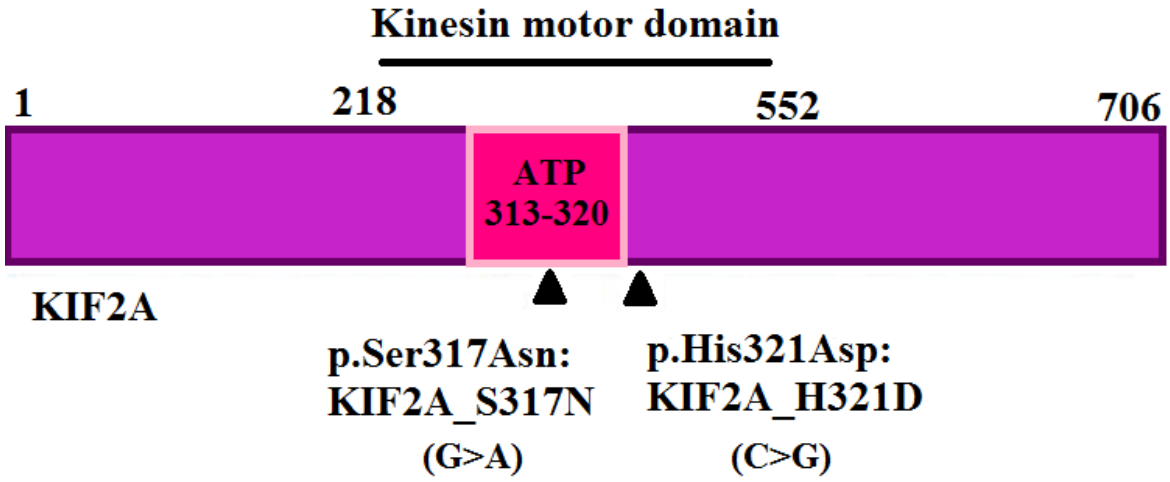

Figure 2.3: Schematic representation of KIF2A that shows the locations of two heterozygous mutations that causes MCD (Adapted from [9]).

Chapter 3

MATERIAL AND METHODS

3.1 Site-directed mutagenesis of *Kif2a*

Missense point mutations were created by site-directed mutagenesis. PCR reaction mixture contained 1X Phusion HF reaction buffer (New England BioLabs, Cat. #B0518S), 200 µM dNTP's, 0.5µM forward primer and 0.5µM reverse primers (Appendix C), 3% DMSO, 10ng pEGFP-C1-Kif2a.1 as DNA template and 1 Unit Phusion Hot Start Flex DNA Polymerase (New England BioLabs, Cat. #M0535L). PCR conditions for denaturing, annealing and extension steps were 98^{o}C for 45 seconds, 60^{o}C for 2 minutes and 72^{o}C for 7 minutes, respectively for 25 cycles. PCR products were purified by using EZ-10 Spin Column PCR Products purification kit (Bio Basic Canada Inc., Cat. #BS364). DNA concentrations were measured by NanoDrop2000c (Thermo Scientific). PCR products were phosphorylated at 5' 50 µl mixture containing 1mM ATP (New England BioLabs, Cat. #P0756S), 1X Polynucleotide Kinase Buffer A (Fermentas, Cat. #00048086), 10 Unit Polynucleotide Kinase (Thermo Scientific, Cat. #EK0032), and 50 ng purified PCR product was incubated at 37^{o}C for 60 minutes. PNK enzyme was deactivated at 65^{o}C for 25 minutes. To circularize the products, ligation reaction was carried out in 20 µl reaction mixture containing 1X T4 Ligation Buffer (Thermo Sicentific, Cat. #B69), 2.5 Unit T4 DNA Ligase (Thermo Sicentific, Cat. # EL0011) and 5 µl of phosphorylation reaction product at room temperature for 2 hours.

The ligation products were transformed into chemically competent DH5α *Escherichia coli* cells by heat shock method. Briefly, 1 µl of ligation product was added into cells and mixture was incubated on ice for 10 minutes and then 42^{o}C for 1 minute. 500 µl of Luria broth (LB) medium was added onto cells and cells were incubated at 37^{o}C for 1 hour. Cells were plated on LB-kanamycin agar plate since vector had a kanamycin resistant gene. Single colonies were picked and miniprep cultures were incubated at 37^{o}C overnight. Plasmid DNA's were purified by GeneJET Plasmid Miniprep Kit (Thermo Scientific, Cat. #K0503). Concentrations were measured using NanoDrop2000c, 5 µl of miniprep DNA were sent for direct sequencing for validation.

3.2 Coating of plates

500 µl of coating solution (1mg Poly-D-Lysine Hydrobromide (Sigma Life Sciences, Cat. #P9155), 0.1 mg mouse laminin (Millipore, Cat. #CC905) in 30 ml of 1X PBS) was added for one well of 24-well plate with coverslips. Plates were coated overnight in tissue culture incubator (37^{o}C, 5%CO_2). Plates were washed three times with 1 ml of sterile ddH_2O next day and stored at +4^{o}C for 3 weeks or used immediately.

3.3 Primary neuronal culture preparation

Pregnant females at embryonic day 14-18 were sacrificed by cervical dislocation. Embryos were removed from the female and their cortices were dissected in cold 1X HBSS containing 10 mM HEPES. After dissection, cortices were transferred into an enzyme solution (6.4 mg L-cystine, 400 units of papain) which was prepared in dissociation media (82 mM Na_2SO_4, 30 mM K_2SO_4, 5.8 mM $MgCl_2$, 1mM HEPES pH 7.4, 20 mM glucose, 0.001% phenol red, 0.2 mM NaOH in ddH_2O) and cortices were incubated at 37^{o}C for 10 minutes. Then tissue was transferred into light inhibitor (10 mg BSA and 10 mg trypsin inhibitor in dissociation media, adjusting pH with 0.1M NaOH), incubated at 37^{o}C for 1

minute. After light inhibitor, tissue was transferred into heavy inhibitor (100 mg BSA and 100 mg trypsin inhibitor in dissociation media, adjusting pH with 0.1M NaOH) incubated for 1 minute at 37^{o}C. Tissues were transferred into BME (Lonza, Cat. #BE12-105F) containing 0.5% L-glutamine, 1% P/S and 5% FBS (BF) and washed in BF twice at room temperature. Finally, the tissue was triturated with a 10 ml serological pipette three times and incubated until large clumps settled down. Upper cell suspension was collected without disturbing the clumps and cells were counted with a cytometer. 300.000 cells were plated per well of 24-well plate in 500 µl BF volume. Two hours later, medium was aspirated and 500 µl of N-2 (Gibco Life Technologies, Cat. #17502-048) and B-27 (Gibco Life Technologies, Cat. #12587-010) supplemented fresh BF media (BNBF) was added per well.

3.4 Transfection of Neuro2A cell line by using Lipofectamine® 2000 reagent

Neuro2A cell line (N2A) was grown in MEM (Gibco Life Technologies, Cat. #31095029) that contained 5% FBS (HyClone), 1% P/S (Gibco Life Technologies, Cat. #15140122) and 0.5% L-Glutamine (HyClone). When the confluency of the cells reached to 70%, transfection was done. 2 µl of Lipofectamine® 2000 reagent was added onto 50 µl of Opti-MEM®I and 2 µg of DNA was added onto 50 µl of Opti-MEM®I for one of 24-well plate that contained coverslip or 6 µl of Lipofectamine® 2000 reagent was added onto 150 µl of Opti-MEM®I and 4 µg of DNA was added onto 150 µl of Opti-MEM®I for one of 6-well plate and incubated for 5 minutes at room temperature After incubation, Lipofectamine® 2000-Opti-MEM®I and DNA-Opti-MEM®I were mixed with each other and incubated at room temperature for 20 minutes. 100 µl of the mixture was added onto one well of 24-well plate or 300 µl of mixture was added onto one well of 6-well plate. Then plate was put in tissue culture incubator.

3.5 Transfection of primary neuronal culture by using Lipofectamine® 2000 reagent

Two days after preparing the primary neuronal culture, media in the wells (24-well plate) –conditioned media- were collected and saved at 37^{o}C. 500 µl of Opti-MEM®I was added into each well and plate was returned to tissue culture incubator. 2 µl of Lipofectamine® 2000 reagent was added onto 250 µl of Opti-MEM®I and 1µg of DNA was added onto 250 µl of Opti-MEM®I for one of 24-well plate that contained coverslip and incubated for 10 minutes at room temperature. After incubation, Lipofectamine® 2000-Opti-MEM®I and DNA-Opti-MEM®I were mixed with each other and incubated at room temperature for 20 minutes. 500 µl of the mixture was added onto one well of 24-well plate and incubated in tissue culture hood for 2 hours. Media in the wells were aspirated and 500 µl of 50% conditioned medium and 50% fresh BNBF was added onto each well.

3.6 Immunofluorescence of primary neuronal cultures and Neuro2A cell line

Two days after transfection for both primary neuronal culture and Neuro2A cell line, 500µl of 4% Paraformaldehyde (dissolved in ddH_2O with heating and stirring, adjusted pH to 7.2) was added to wells containing cells in media very slowly under hood and incubated at room temperature for 20 minutes. PFA was aspirated and then wells were washed with 1X cold PBS for one minute twice.

Coverslips were placed parafilm inside a staining chamber. Each coverslip was blocked with blocking solution (3% BSA, 0.5% TritonX-100 in 1X PBS) for 45 minutes at room temperature. After blocking, coverslips were incubated with 50µl of primary antibody diluted in blocking solution for 2 hours at room temperature. Dilution ratios are indicated in Table 3.1. Coverslips were washed with 50 µl of 1X cold PBS for 5 minutes 3 times. After washing, coverslips were incubated with 50 µl of secondary antibody for 1 hour at room temperature in dark. Coverslips were washed with 50 µl of 1X PBS for 5 minutes in dark and then incubated with 50 µl of DAPI (diluted 1:1000 in 1X PBS) for 10 minutes in dark. Coverslips were washed with 50 µl of 1X cold PBS for 5 minutes two times in dark. Coverslips were mounted using mounting media (Thermo Scientific, Cat. #TA-060-UG). Immunofluorescent images were captured using Nikon Eclipse 90i confocal microscope and NIS-Elements AR software.

Table 3.1: Primary Antibodies used in immunofluorescence

Antibody	**Host**	**Company**	**Catalogue Number**	**Dilution**
GFP	Rabbit	Santa Cruz	sc-8334	1:1000
GFP	Chick	Aves Labs	GFP-1020	1:800
myc	Mouse	Santa Cruz	sc-40	1:1000
Kif2a	Rabbit	Abcam	ab37005	1:5000
βIII Tubulin (Tuj1)	Mouse 2b	Abcam	ab7751	1:500
Tubulin	Rat	Abcam	ab6160	1:500
Detryrosinated alpha Tubulin	Rabbit	Abcam	ab48389	1:200

Table 3.2: Secondary Antibodies used in immunofluorescence

Antibody	**Host**	**Company**	**Catalogue Number**	**Dilution**
Donkey Anti-Mouse IgG (H+L) Alexa Fluor®488	Mouse	Invitrogen	A21202	1:2000
Donkey Anti-Rabbit IgG (H+L) Alexa Fluor®488	Rabbit	Invitrogen	A21206	1:2000
Goat Anti-Chick IgG (H+L) Alexa Fluor®488	Chick	Life Technologies	A11039	1:1000
Donkey Anti-Rabbit IgG (H+L) Alexa Fluor®594	Rabbit	Invitrogen	A21207	1:1000
Goat Anti-Rat IgG (H+L) Alexa Fluor®594	Rat	Abcam	ab150160	1:1000
Streptavidin Alexa Fluor®594 conjugate	-	Life technologies	S32354	1:5000

3.7 Cloning of *Kif2a.1, Kif2a.2* and *Kif2a_H321D* into BirA* vector

pcDNA3.1(-)mycBirA (BirA*, N terminal) vector was a kind gift of Dr. Elif Nur Fırat Karalar. *Kif2a.1, Kif2a.2* and *Kif2a-H321D* were subcloned from pEGFP-C1 vector into pcDNA3.1(-)mycBirA vector. PCR was set up in 30 µl reaction mixture containing 1X Phusion HF reaction buffer, 300 µM dNTP's, 0. 5µM forward primer and 0.5µM reverse primers (Appendix C), 150 ng pEGFP-C1-Kif2a.1, pEGFP-C1-Kif2a.2 or pEGFP-C1-Kif2a-H321D as DNA template and 1 Unit Phusion Hot Start Flex DNA Polymerase (New England BioLabs, Cat. #M0530L). PCR conditions for denaturing, annealing and extension were 98^{o}C for 15 seconds, 59^{o}C for 30 seconds and 72^{o}C for 1.5 minutes, respectively for 30 cycles. PCR products were run on agarose gel and the correct band was excised under UV light and DNA extraction from agarose gel was performed by using EZ-10 Spin column DNA Gel Extraction Kit (Bio Basic Canada Inc., Cat. #BS353). Forward primer contained XhoI restriction enzyme site and reverse primer contained EcoRI restriction enzyme site. Restriction enzyme digestion was set up in 20 µl reaction mixture containing 2X Tango Buffer, 5 Unit XhoI (Thermo Scientific, Cat. #ER0691), 5 Unit EcoRI (Thermo Scientific, Cat. #ER0271) and 10 µl gel purified PCR product and 0.5 µl of pcDNA3.1(-)mycBirA plasmid DNA. Samples were double-digested at 37^{o}C overnight with XhoI and EcoRI. Next day, dephosphorylation was carried out with 1 µl of FastAP (Alkaline phosphatase) (Thermo Scientific, Cat. #EF0651) to prevent self-ligation of the plasmid DNA. PCR products and plasmid DNA were purified with PCR purification kit. pcDNA3.1(-)mycBirA vector was ligated with PCR products in a 10 µl reaction mixture containing, 1X T4 Ligase Buffer, 5 Unit T4 ligase and incubated at room temperature for 2 hours.

1 µl of ligation product was transformed into chemically competent DH5α *E.coli* cells by heat shock method. Cells were plated on LB/ampicillin plates by using spread plate technique. Single colonies were picked and miniprep cultures were incubated at 37^{o}C

overnight with constant shaking and plasmid DNA's were purified by GeneJET Plasmid Miniprep Kit. Diagnostic digestion was set up in 20 µl reaction mixture containing 1µl of DNA, 1X NEB 3 Buffer (New England Biolabs, Cat. #B7003S), 10 Unit EcoRI (New England Biolabs, Cat. #R0101S), 5 Unit XhoI (New England Biolabs, Cat. #R0146S). Samples were double digested at 37^{o}C for 2 hours and run on agarose gel to confirm that selected colonies had correct size insert. Concentrations were measured by using NanoDrop2000c and 5 µl of miniprep DNA were sent to direct sequencing for validation. After confirming that miniprep DNA had correct insertions, maxi-prep cultures were incubated at 37^{o}C overnight with constant shaking and plasmid DNA that contained *Kif2a.1*, *Kif2a.2* and *Kif2a-H321D* separately were purified with PureLink™ HiPure Plasmid Maxiprep Kit.

3.8 Transfection of Neuro2A cell line by using Polyethylenimine reagent

Neuro2A cell line (N2A) was grown in MEM that contained 5% FBS, 1% P/S and 0.5% L-Glutamine. Transfection was performed at 70% confluency using 1mg/ml Polyethylenimine (PEI) dissolved in sterile ddH_2O (Polysciences Inc, Cat. #23966). Cells were washed with 1X PBS and warm (37^{o}C) MEM medium (5ml for 60mm plate or 10ml for 10cm plate) containing 5% FBS and 0.5% L-Glutamine was added on cells and plates were replaced into tissue culture incubator. 4 µg DNA and 12 µl of PEI were added into 1ml of Opti-MEM®I for 60 mm plate and 60 µg DNA and 180 µl PEI were added into 3 ml of Opti-MEM®I for 10 cm plate. Mixture was vortexed for 30 seconds and incubated for 40 minutes at room temperature. After incubation, transfection mixture was added on cells dropwise and plates were put into tissue culture incubator for 6 hours. After incubation, medium was aspirated from plates and complete MEM medium (5% FBS, 1% P/S and 0.5% L-Glutamine) was added onto cells (5 ml for 60 mm plate and 10 ml for 10 cm plate).

3.9 Biotin treatment of cultures

One day after transfection, media of the cells were aspirated and fresh media containing 0.05 μM D-biotin (Molecular Probes by Life technologies, Cat. #B-1595, 0.5 g D-biotin was dissolved in 4.1 ml DMSO) was added. Plates were returned to the tissue culture incubator overnight.

3.10 Affinity purification of biotinylated proteins by streptavidin beads

One day after biotinylation, medium was aspirated and cells were washed with 1X PBS twice. Lysis buffer (50 mM Tris-HCl pH 7.4, 500 mM NaCl, 0.2% w/v SDS in ddH_2O, 1X protease inhibitor (Thermo Scientific, Cat. #1862209) or 1 tablet of protease inhibitor cocktail (Roche Complete Mini, EDTA-free) per 10 ml lysis buffer and 1mM DTT (Roche, Cat. #05091284001) was added onto cells and cells were gently harvested at room temperature. Lysate was transferred into 15ml conical tube. 1.2 ml 20% Triton X-100 dissolved in ddH_2O per 10 cm plate (AppliChem, Cat. #A1388,0500) was added. Sonication (Bandelin Sonoplus HD2070) was applied for 10 seconds, 3 cycles, one session for 60 mm plate and 30 seconds, 3 cycle, two sessions for 10 cm plate at cold room and samples were put on ice after each session. Prechilled 50 mM Tris-HCl pH 7.4 was added into tubes. Sonication was applied again for 30 seconds, 3 cycles, one session for 60 mm plate and 10 seconds, 3 cycle, three sessions for 10 cm plate at cold room and samples were put on ice after each session. Samples were aliquot evenly into prechilled 1.5 ml centrifuge tubes and centrifuged at 16,500xg for 10 minutes at 4^oC.

During the sample centrifugation, fresh 15 ml conical tubes were placed and room-temperature lysis buffer and room-temperature 50 mM Tris-HCl pH 7.4 was added onto each tube. Stock Pierce® Streptavidin Plus UltraLink® Resin (Thermo Scientific, Cat. #53117) beads were mixed with the solution that contained lysis buffer and Tris-HCl pH 7.4 (5 μl beads for the cells that harvested from 60 mm plate and 15 μl beads for the cells

that harvested from one 10 cm plate). Beads were washed by rotating for 3 minutes at room temperature. After centrifugation at 3900xg for 2 minutes, supernatant was removed carefully without disturbing the beads. After sample centrifugation, 50 µl of the supernatant was transferred into new 1.5 ml centrifuge tubes as 'input'. Rest of the supernatant was transferred to the tubes containing beads. Tubes were incubated at cold room on a rotator overnight.

Next day, tubes were centrifuged at 3900xg for 2 minutes and 50 µl of supernatant was collected into new 1.5 ml centrifuge tube as 'supernatant after pull down'. Rest of the supernatant was discarded. Wash Buffer I (2% SDS) was added into tubes and tubes were placed on rotator for 8 minutes at room temperature. Beads were washed with Wash Buffer I twice. After removing supernatant, Wash Buffer II (0.1% w/v deoxycholic acid, 1% w/v Triton X-100, 1 mM EDTA, 500 mM NaCl, 50 mM HEPES pH 7.5) was added and tubes were placed on rotator for 8 minutes at room temperature. Wash Buffer III (0.5% w/v deoxylic acid, 0.5% w/v NP-40, 1 mM EDTA, 250 mM LiCl, 10 mM Tris-HCl pH 7.4) was added into tubes and tubes were placed on rotator for 8 minutes at room temperature. 50 mM Tris-HCl pH 7.4 was added into tubes and tubes were placed on rotator for one minute at room temperature. 5% of beads were saved into a new 1.5 ml centrifuge tubes for pulldown verification. Tubes that contain beads and 50 mM Tris-HCl pH 7.4 were centrifuged and supernatant was removed. 50 µl of 50 mM ammonium bicarbonate was added to the tubes, re-suspend gently and store at 4^{o}C then they were analyzed by mass spectrometry.

3.11 SDS-PAGE

A 5% stacking SDS-PAGE gel (5% Acrylamide-Bisacrylamide (29:1), 126 mM Tris-HCl pH 6.8, 0.1% SDS, 0.1% APS, 0.1% TEMED) was added on top of either 7.5% separating SDS-PAGE gel (7.5% Acrylamide-Bisacrylamide (29:1), 375 mM Tris-HCl pH 8.8, 0.2% SDS, 0.2% APS, 2.5% TEMED) for KIF2A western blot analysis or 10% separating SDS-PAGE gel (10% Acrylamide-Bisacrylamide (29:1), 375 mM Tris-HCl pH 8.8, 0.2% SDS, 0.2% APS, 2.5% TEMED). 7.5 μg – 10 μg proteins were mixed with 2X SDS-Sample Buffer (100mM Tris-HCl pH 6.8, 20% glycerol, 4% SDS, 0.02% bromophenol blue, 2% β-mercaptoethanol). Samples were boiled at 95^{o}C for 5 minutes and loaded into wells. Broad-Way Multi™ Prestained Protein Marker (iNtRON Biotechnology, Cat. #24085) was used. Samples were run at 90V for 1 hour, 100V for one hour and 120V for 20 minutes in 1L of 1X SDS Running Buffer pH 8.3 (10X, 30 g Tris Base, 187.6 g Glycine, 1% SDS in total volume of 1L). Gels were used for either western blot analysis or silver staining procedure.

3.12 Western blotting

By using wet-transfer method (1.45g Tris Base, 7.25g Glycine, 150ml Methanol in total volume of 1L), proteins that were on SDS gels were transferred onto a PVDF -polyvinyl difluoride membrane- (Thermo Scientific, Cat. #88518). Wet-transfer was done at cold room either at 55 mA overnight or at 90mA 2 hours. After transfer, membrane was incubated in blocking buffer (5% Nonfat Dried Milk Powder (AppliChem, Cat. #A0830) in TBS-T (10mM Tris-HCl, 150mM NaCl, 0.05% Tween)) for 45 minutes to 1 hour. Membrane was incubated with primary antibody diluted in either blocking buffer or 2% BSA -Bovine Serum Albumin- (SantaCruz Biothecnology Inc., Cat. #sc-2323A) in TBS-T or blocking buffer for either 2 hours at room temperature or overnight at cold room. Membrane was washed with TBS-T for 15 minutes three times at room temperature.

Incubation of membrane with secondary antibody diluted in blocking buffer was done for 1 hour at room temperature. Membrane was washed with TBS-T for 15 minutes 3 times at room temperature. Membrane was incubated in Western Bright™ Sirius western blotting detection kit (Advansta, Cat. #K-12043-D20) for 4 minutes at room temperature. Membrane was visualized under Gel Logic 2200 Imaging system (Molecular Imaging System CareStream Health Inc.)

Table 3.3: Primary Antibodies used in western blotting

Antibody	Host	Company	Catalogue Number	Dilution
myc	Mouse	Santa Cruz	sc-40	1:1000
Biotin	Rabbit	*	-	1:20000
Radford	Human	**	-	1:10000
Beta-Actin	Rabbit	Thermo Scientific	PA5-16914	1:2500
Histone H3	Rabbit	Cell Signalling	9715	1:2500
* Homemade antibody was a kind gift of Dr. Nurhan Özlü ** Human anti-sera was a kind gift of Dr. Robert Darnell, Rockefeller University				

Table 3.4: Secondary Antibodies used in western blotting

Antibody	Host	Company	Catalogue Number	Dilution
Anti-Mouse IgG HRP-linked	Mouse	Cell Signalling	7076S	1:2500
Anti-Rabbit IgG HRP-linked	Rabbit	Cell Signalling	7074S	1:2500
Goat Anti-Human IgG (H+L) HRP-linked	Human	Thermo Scientific	31412	1:5000

3.13 Rapid silver staining

After preparing SDS-PAGE gel (10% separating gel on top of 5% stacking gel), 7.5 µg – 10 µg of proteins were mixed with SDS-Sample Buffer. Samples were boiled at 95^{o}C for 5 minutes and loaded into wells. Samples were run at 90V for 1 hour, 100V for one hour and 120V for 20 minutes in 1L of 1X SDS Running Buffer pH 8.3. Gel was incubated in 50 ml of formaldehyde fixing solution (40%v/V methanol, 37% formaldehyde, 60% ddH_2O) for 1.5 hour at room temperature. Gel was washed with ddH_2O for 10 minutes three times. Gel was soaked in 0.002% sodium thiosulfate (30 mg in 150 ml ddH_2O), then was washed with ddH_2O for 20 seconds three times. Gel was soaked in 50 ml of cold 0.1% silver nitrate (0.05g in 50 ml ddH_2O, 10 µl of 37% formaldehyde was added freshly) for 20 minute agitating slowly in cold room. Gel was washed with ddH_2O and then 10 ml of thiosulfate developing solution (3% w/v sodium carbonate, 0.0004% w/v sodium thiosulfate in 500 ml ddH_2O, add 250 µl 37% formaldehyde freshly). Gel was soaked in 50 ml of fresh thiosulfate developing solution and agitating slowly until band intensities were adequate. Gel was soaked in thiosulfate developing solution that contained 5% acetic acid for 10 minutes at room temperature and washed with ddH_2O for 10 minutes at room temperature. Photo of the gel was taken and gel was soaked in 10% acetic acid to store at +4^{o}C.

Chapter 4

RESULTS

4.1 Localization and Expression of KIF2A.1, KIF2A.2, and KIF2A.3 in Neuro2A cell line and primary neuronal cultures

Kif2a.1, Kif2a.2 and Kif2a.3 were transfected into both Neuro2A cells and E18 primary neuronal cultures to observe if there is a change in the localization of different KIF2A isoforms. All KIF2A isoforms were cloned into pEGFP_C1 backbone vector and were expressed as GFP fusion protein. Two days after transfection, cells were fixed and immunostained with an antibody against GFP. Primary neurons were also co-stained with an antibody against the neuronal tubulin Tuj1 (beta-III tubulin). Cell nuclei were imaged with DAPI stain. GFP positive cells were the cells that were transfected successfully and expressed the KIF2A isoforms. Both GFP positive and Tuj1 double positive neurons were selected and imaged under confocal microscope. Immunofluorescence results demonstrated that the localization of different KIF2A isoforms were the same, they were both cytoplasmic and nuclear in Neuro2A cells (Figure 4.1) and E18 primary neurons (Figure4.2).

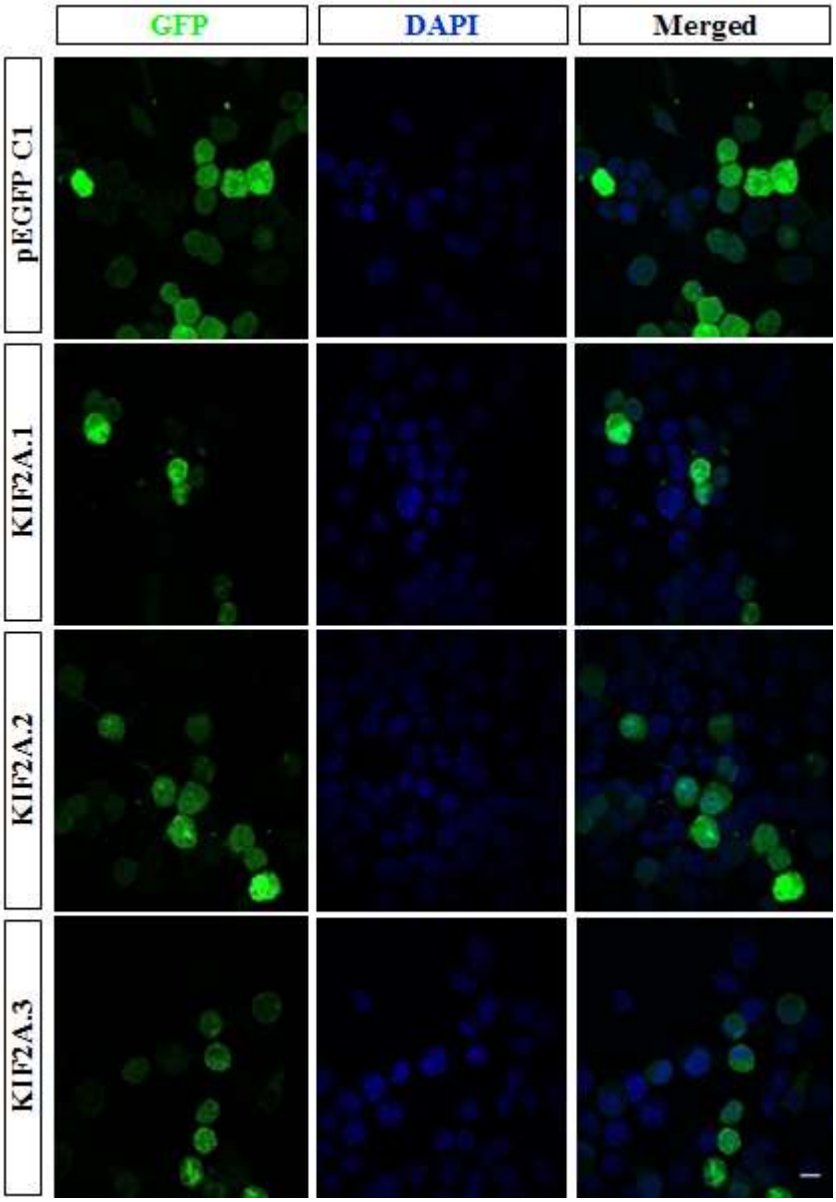

Figure 4.1: Immunofluorescence staining of KIF2A-GFP (green) and DNA (blue) in Neuro2A cells that were transfected with backbone vector pEGFP_C1 or three KIF2A isoforms (KIF2A.1, KIF2A.2 and KIF2A.3) separately. All KIF2A isoforms were localized to both nucleus and cytoplasm. Scale bar, 10μm.

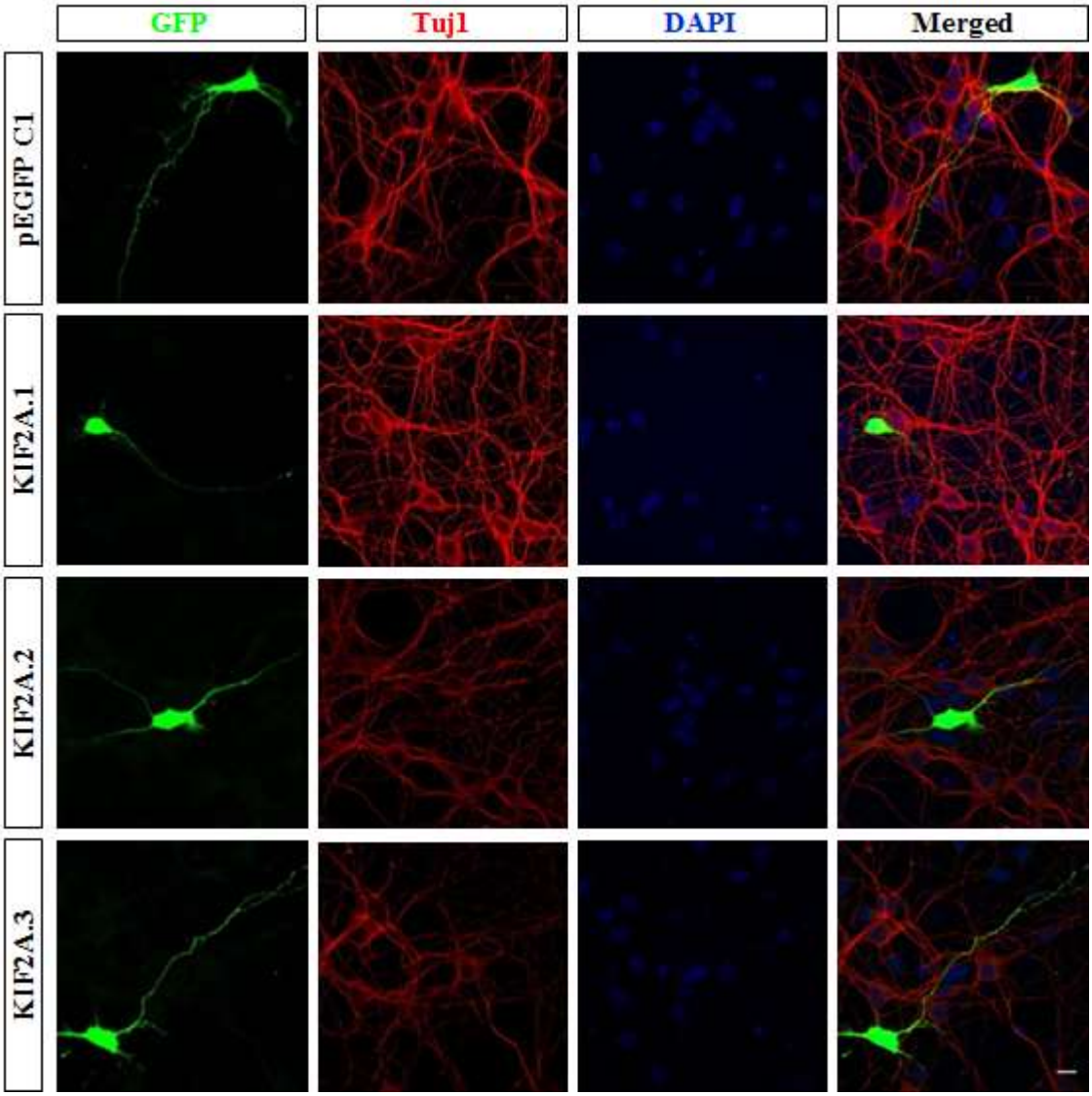

Figure 4.2: Immunofluorescence staining of KIF2A-GFP (green), Tuj1 (red) and DNA (blue) in E18 primary neurons that were transfected with pEGFP_C1 or three KIF2A isoforms (KIF2A.1, KIF2A.2 and KIF2A.3) separately. All KIF2A isoforms were localized to both nucleus and cytoplasm. Scale bar, 10μm.

4.2 Co-localization of KIF2A.1, KIF2A.2, and KIF2A.3 with stable and dynamic microtubules

Since KIF2A has a role in microtubule depolymerization, we wanted to determine if KIF2A isoforms co-localized with stable and/or dynamic microtubules. All isoforms were overexpressed in E14 primary neuronal cultures by transfection with Lipofectamine2000® reagent. After fixation, they were stained with GFP and markers of stable and dynamic microtubules. An antibody against tyrosinated tubulin was used to detect dynamic microtubules and an antibody against detyrosinated tubulin detected stable microtubules. Results demonstrated that, all KIF2A isoforms are interacting with mainly dynamic microtubules (Figure 4.3 and 4.4) and at least a subpopulation co-localizes with stable microtubules (Figure 4.5 and 4.6).

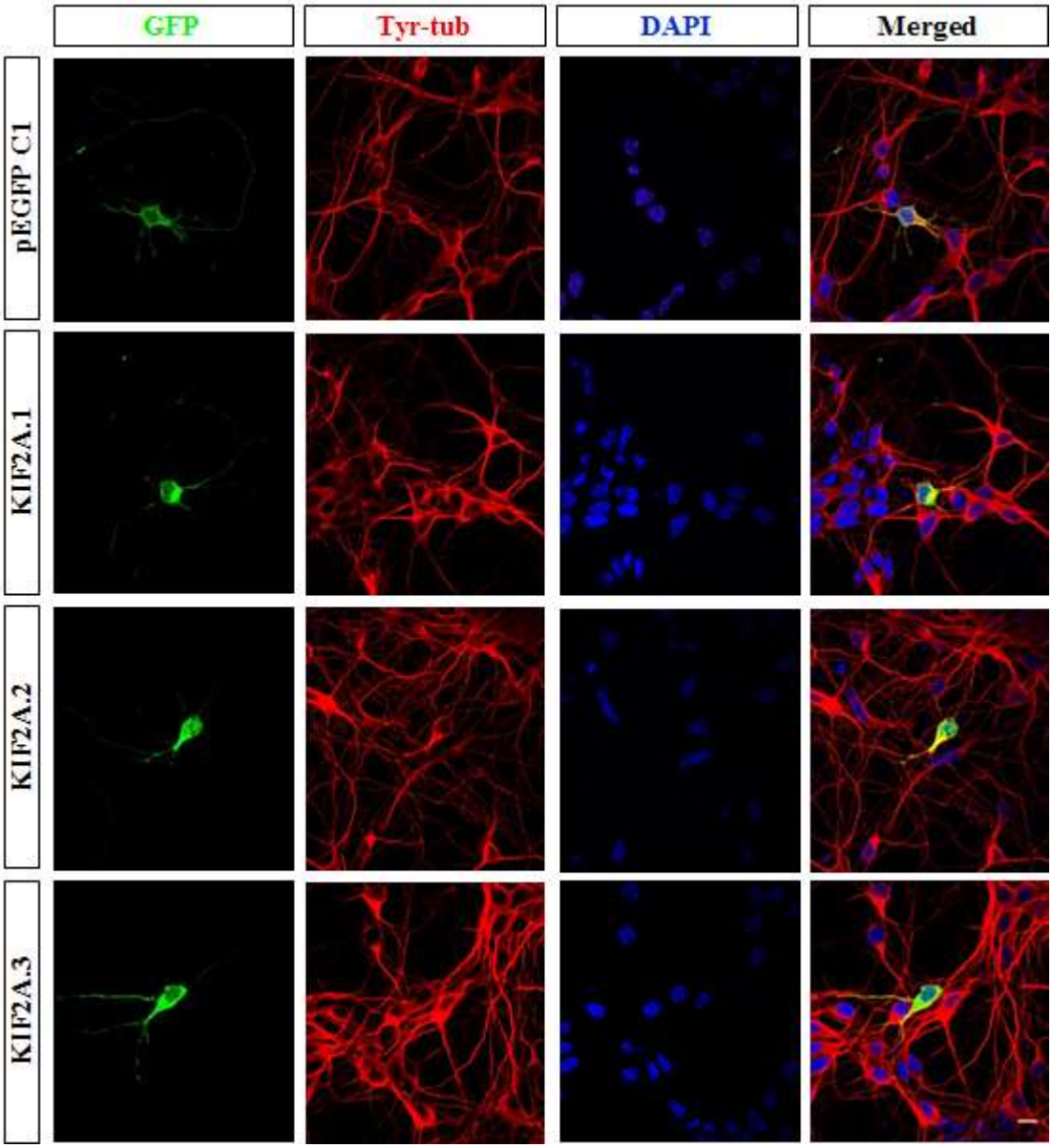

Figure 4.3: Immunofluorescence staining of KIF2A (green), dynamic microtubules (red) and DNA (blue) in E14 primary neurons that were transfected with pEGFP_C1 or one of the three KIF2A isoforms (KIF2A.1, KIF2A.2 and KIF2A.3) separately. Scale bar, 10μm.

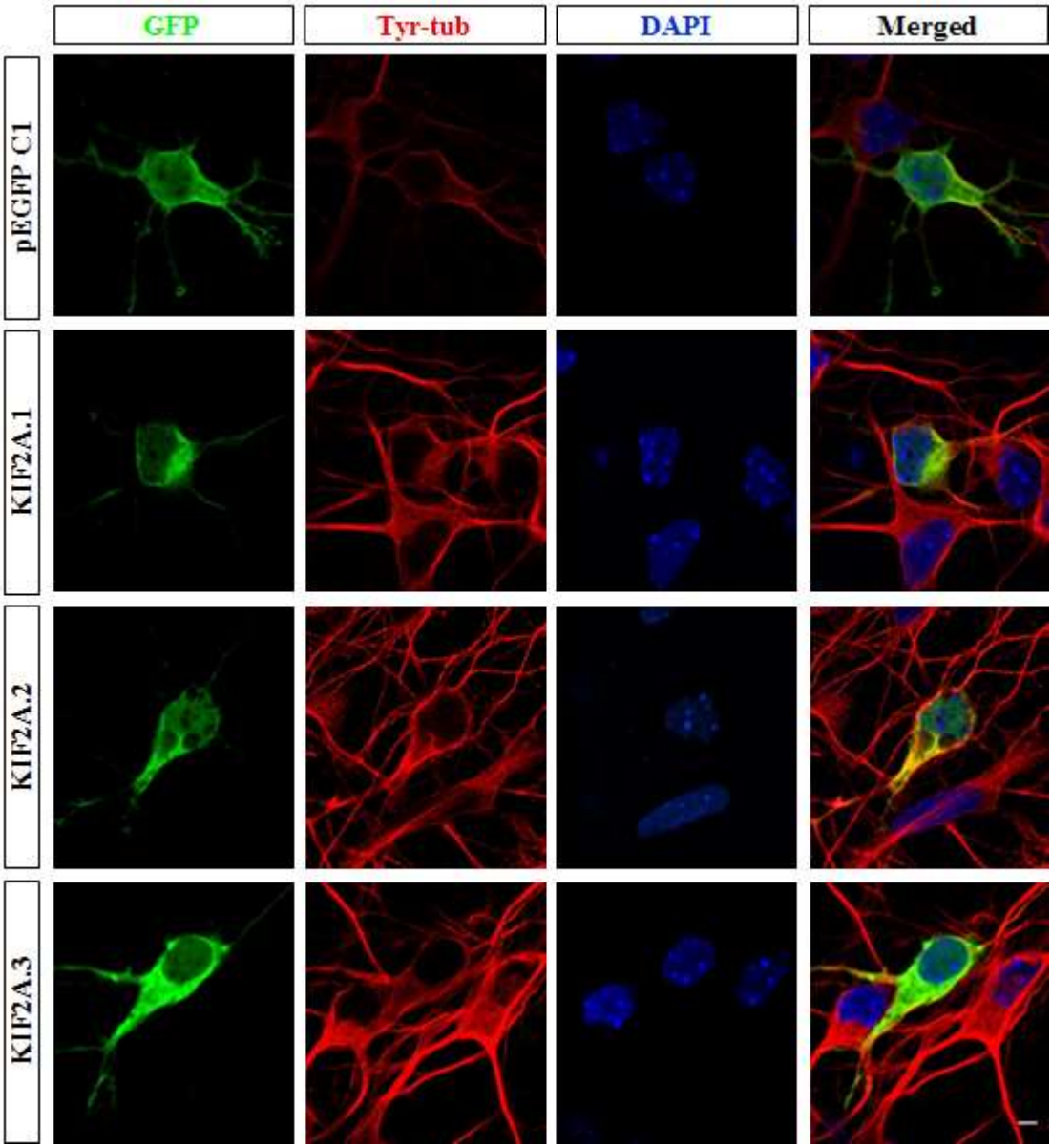

Figure 4.4: Higher magnification image of Figure 4.3. Scale bar, 10μm.

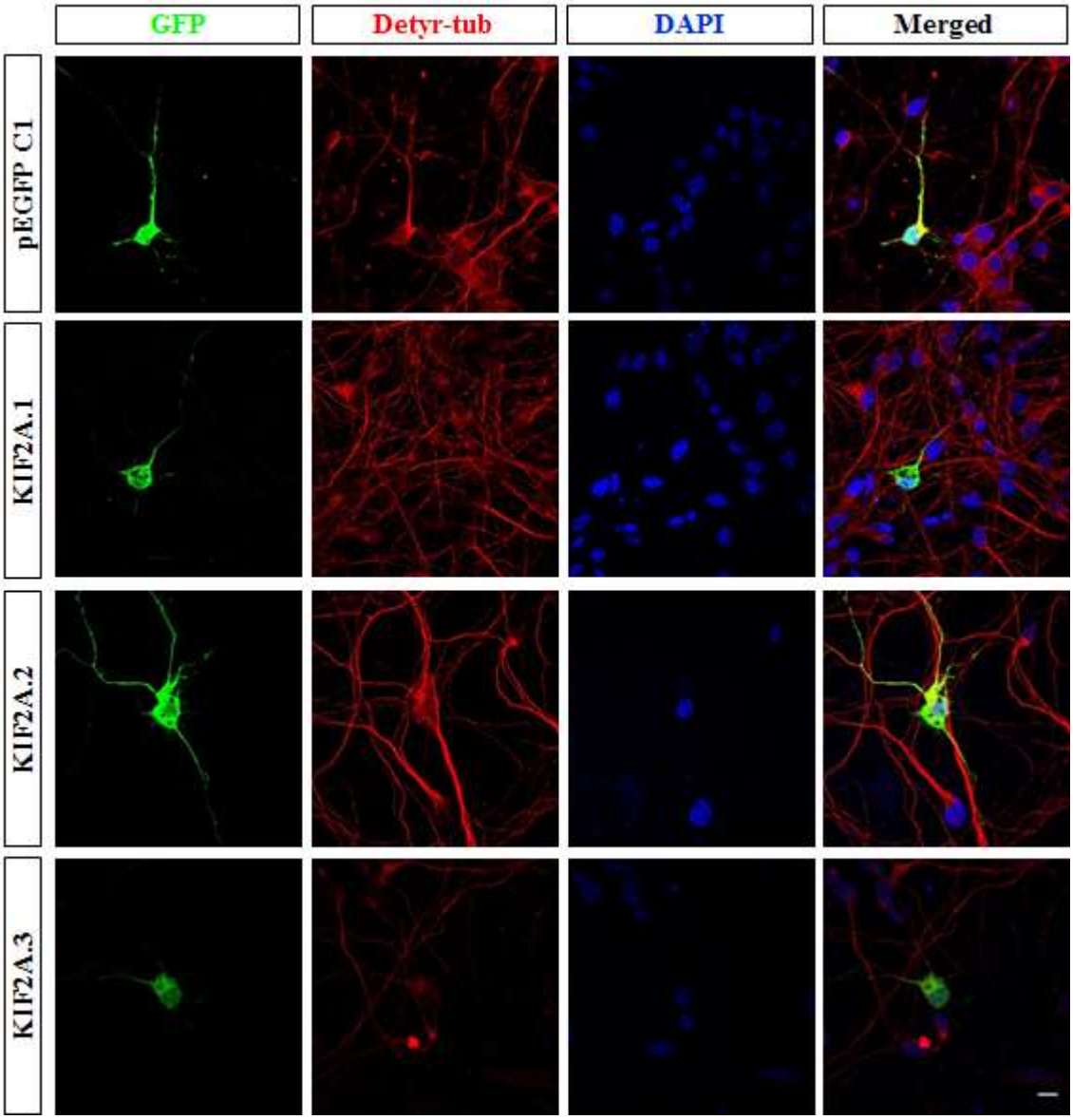

Figure 4.5: Immunofluorescence staining of KIF2A-GFP (green), stable microtubules (red) and DNA (blue) in E14 primary neurons that were transfected with pEGFP_C1 or one of the three KIF2A isoforms separately. Scale bar, 10μm.

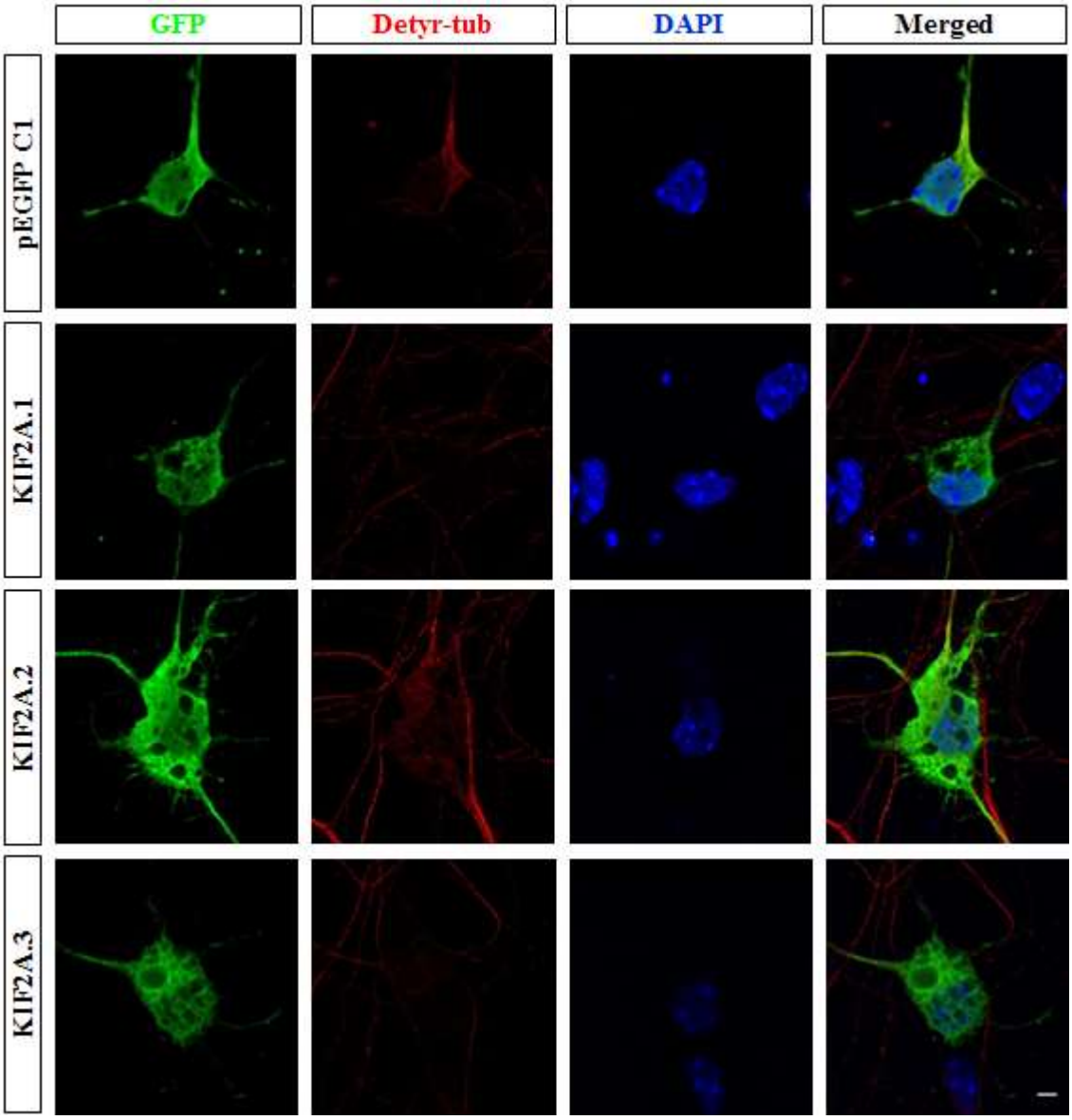

Figure 4.6: Higher magnification image of Figure 4.5. Scale bar, 10µm.

4.3 Effect of KIF2A.1, KIF2A.2, and KIF2A.3 on organelle trafficking

Organelle trafficking in eukaryotic cells is regulated by cytoskeleton-associated motor proteins [43]. Since KIF2A has a role in microtubule depolymerization [11], it might also have a role in organelle trafficking. Mitochondrion was selected as a target organelle. mCherry-TOMM20-N-10 (kind gift from Dr. Cory Dunn, Addgene plasmid #55146) was co-transfected with KIF2A isoforms that were cloned into pEGFP_C1 backbone vector in E14 primary neurons. mCherry-TOMM20-N-10 localizes onto the outer mitochondrial membrane, and is used as mitochondrial marker. After cells were co-transfected, they were fixed with 4% PFA and stained with GFP. mCherry signal was very high and did not need immunofluorescent staining for detection. GFP antibody was used to detect the transfected cells. Immunofluorescence results showed that mitochondria localized mainly to the cytoplasm and also to the apical dendrites of neurons that were transfected with one of the three KIF2A isoforms (Figure 4.7).

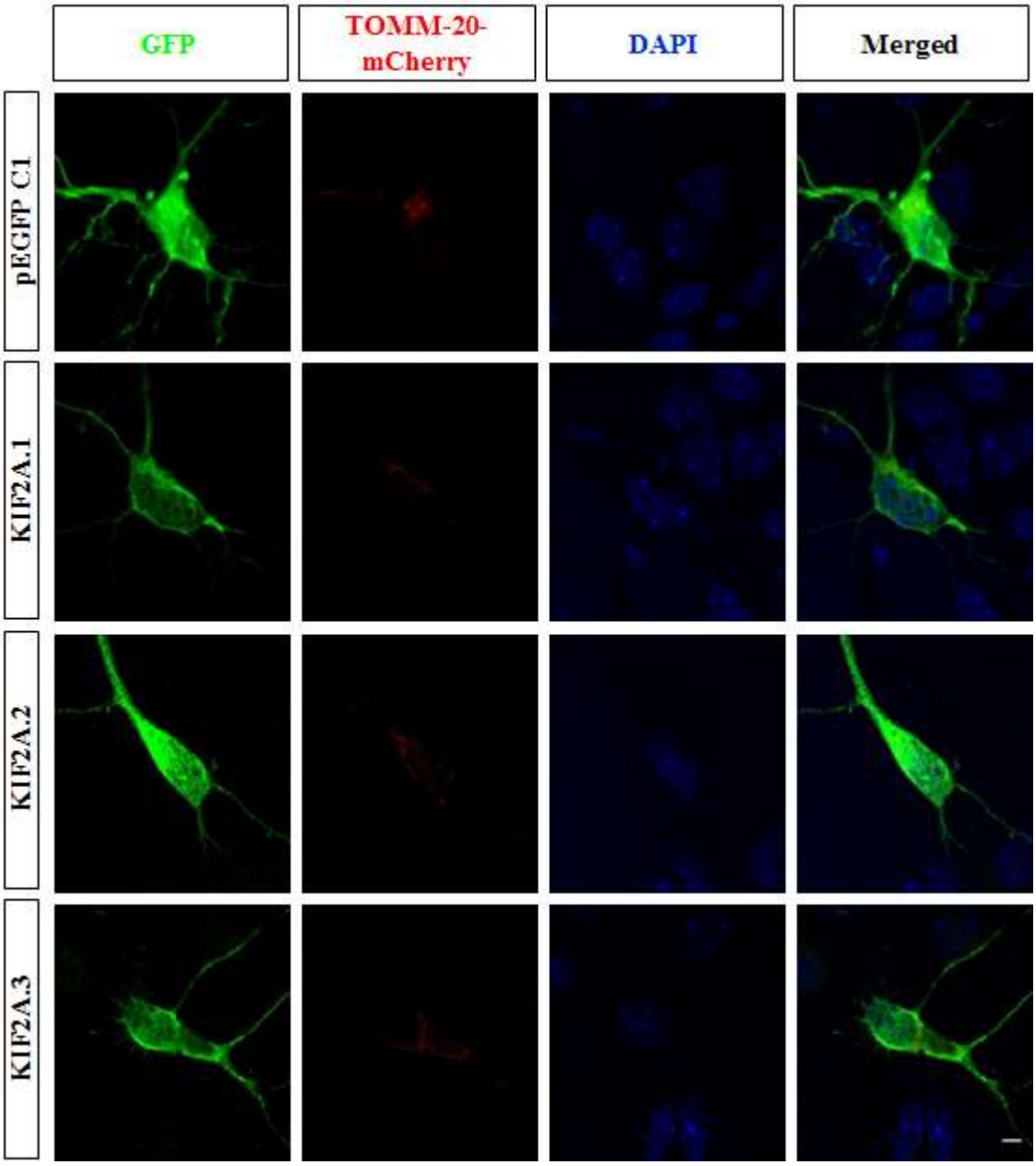

Figure 4.7: : Immunofluorescence staining of KIF2A-GFP (green), mitochondria (red) and DNA (blue) in E14 primary neurons that were transfected with pEGFP_C1 or one of the three KIF2A isoforms (KIF2A.1, KIF2A.2 and KIF2A.3) separately. Scale bar, 10µm.

4.4 Cloning of *Kif2a_S317N* and *Kif2a_H321D* by site-directed mutagenesis

Two different missense point mutations in the *Kif2a* were mapped in two different patients with severe cortical malformations[9]. I tested whether these mutations affected cellular and/or neuronal morphology. The mutated amino acid residues were conserved in mice and mapped onto motor domain of KIF2A protein (Figure 4.8 A). Mutations were created by site-directed mutagenesis using the *pEGFP_C1_Kif2a.1* (Appendix C). After PCR, 5µl of each product was run on 1% agarose gel to verify that PCR worked (Figure 4.8 B). Primers did not contain phosphate group, phosphorylation reaction was carried out and the products were ligated for circularization and transformed into DH5α *E.coli* cells. After colony selection and miniprep culture, samples were double digested to search for an insert. Miniprep samples that contained inserts were sent for direct sequencing and mutagenesis was confirmed (Figure 4.8 C).

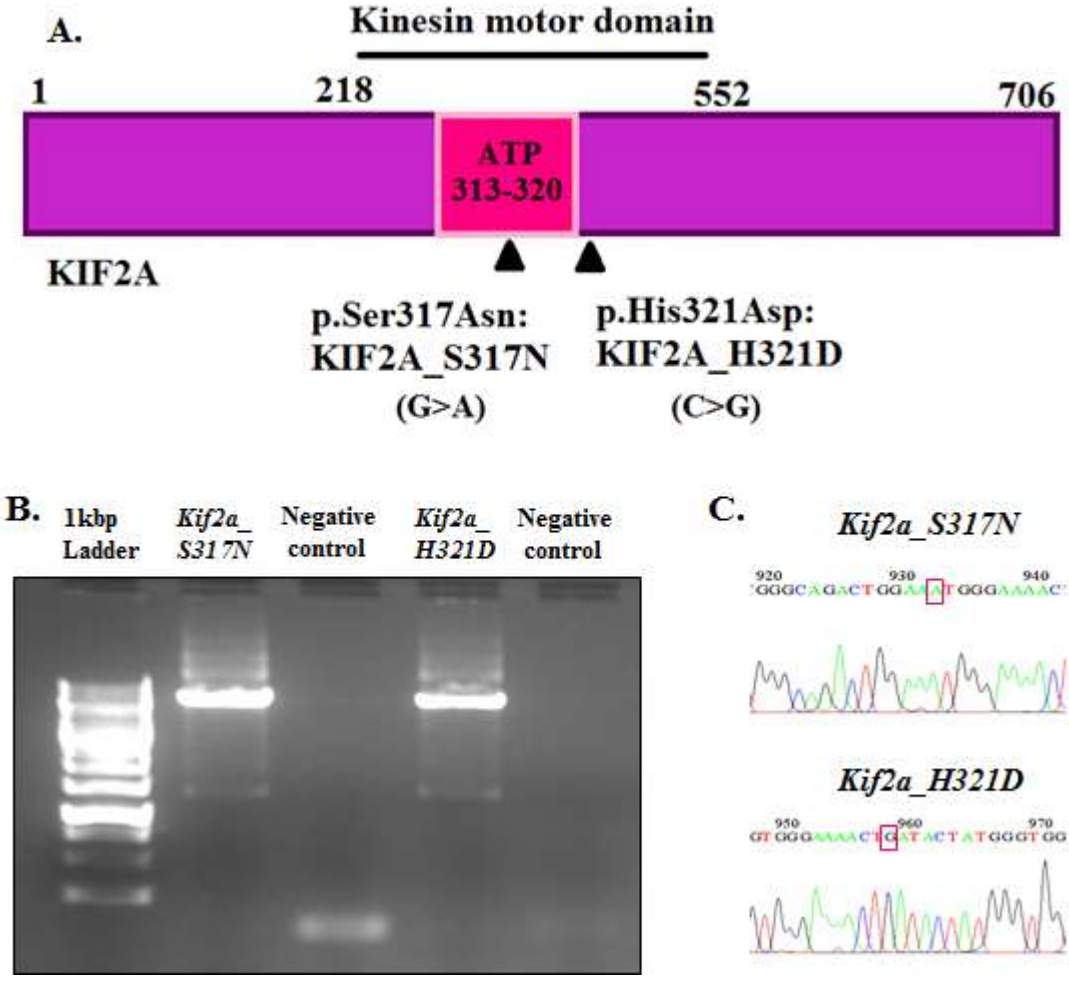

Figure 4.8: A. Schematic representation of KIF2A that shows the locations of two missense point mutations. **B.** Site-Directed mutagenesis PCR was successful. **C.** Point mutations were verified by direct sequencing. Site of the mutations were shown in a box.

4.5 Localization and Expression of KIF2A_S317N and KIF2A_H321D

In order to observe the localization of the mutant KIF2A's, *Kif2a_S317N* and *Kif2a_H321D* were overexpressed in both Neuro2A cells and E18 primary neuronal cultures. Mutant constructs were expressed as a GFP fusion protein (*pEGFP_C1_Kif2a.1*). Two days after transfection, cells were fixed and stained for GFP and DAPI for Neuro2A cells; GFP, Tuj1 and DAPI for E18 primary neurons. Immunofluorescence results demonstrated that the localization of KIF2A_S217N and KIF2A_H321D changed from cytoplasmic and nuclear to only cytoplasmic in Neuro2A cells (Figure 4.9) and E18 primary neurons (Figure 4.11). Moreover, in the mutants, there were cage-like GFP positive structures. To see these cage like structures more clear, higher magnification images were taken for Neuro2A cells (Figure 4.10) and E18 neurons (Figure 4.12).

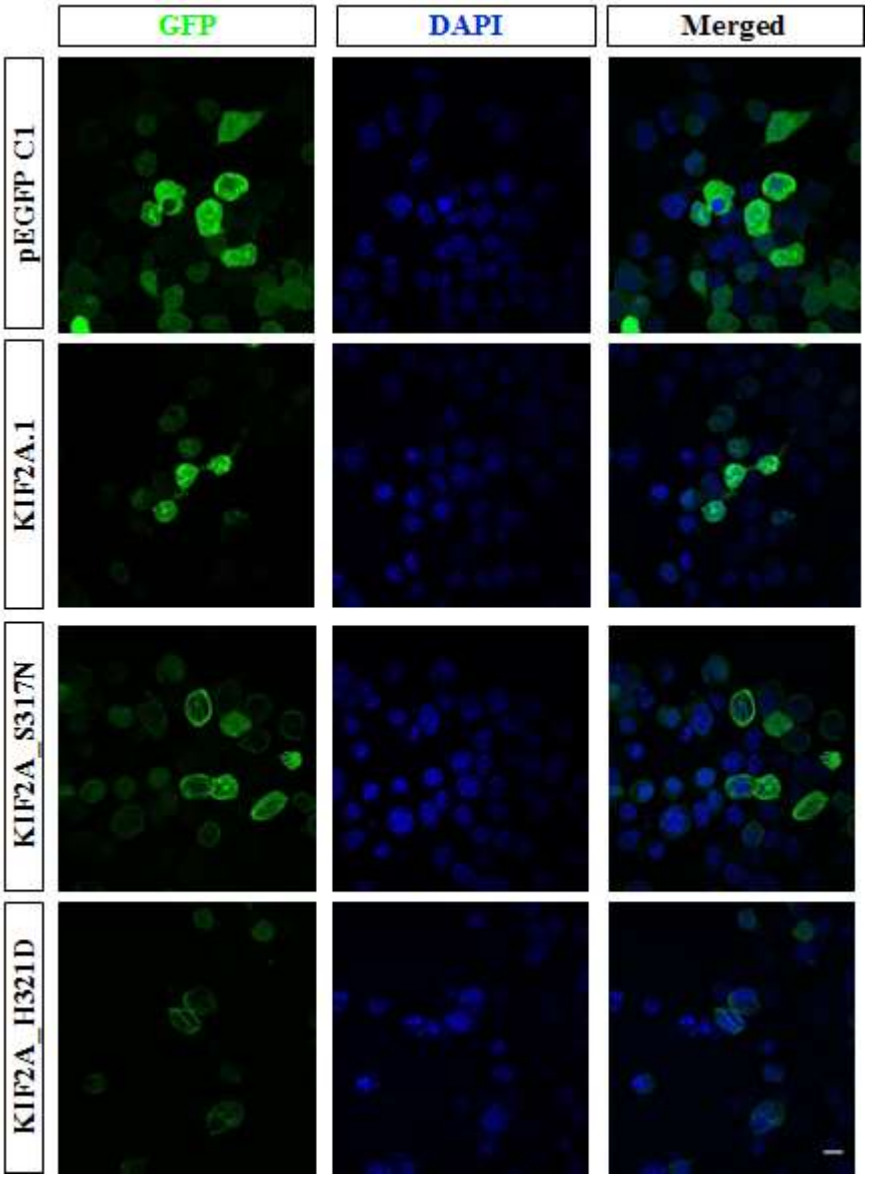

Figure 4.9: Immunofluorescence staining of KIF2A-GFP (green), and DNA (blue) in Neuro2A cells that were transfected with pEGFP_C1 or KIF2A mutants (KIF2A_S317N, KIF2A_H321D) separately. Mutant KIF2A's were localized only to the cytoplasm. Scale bar, 10μm.

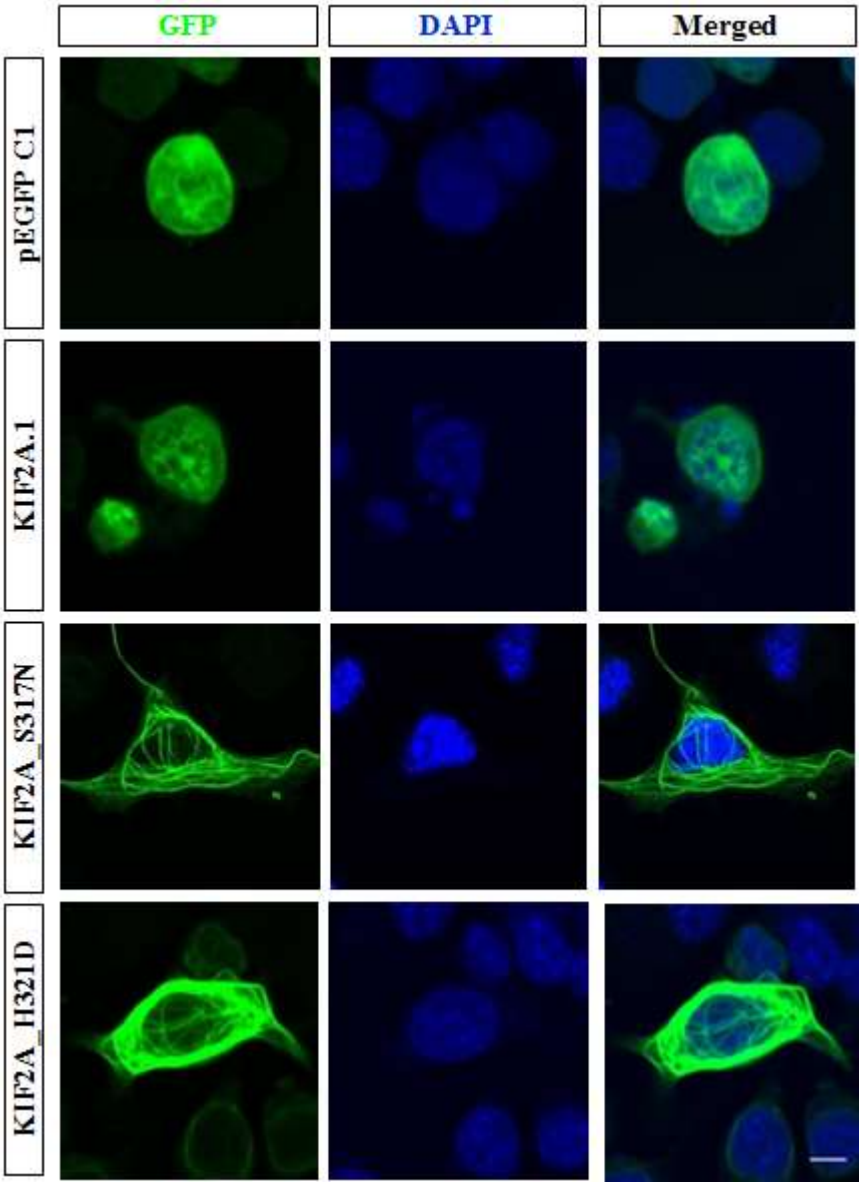

Figure 4.10: Higher magnification image of Figure 4.9 where the cage like structures can be clearly observed in KIF2A_S317N and KIF2A_H321D in Neuro2A cells. Scale bar, 10μm.

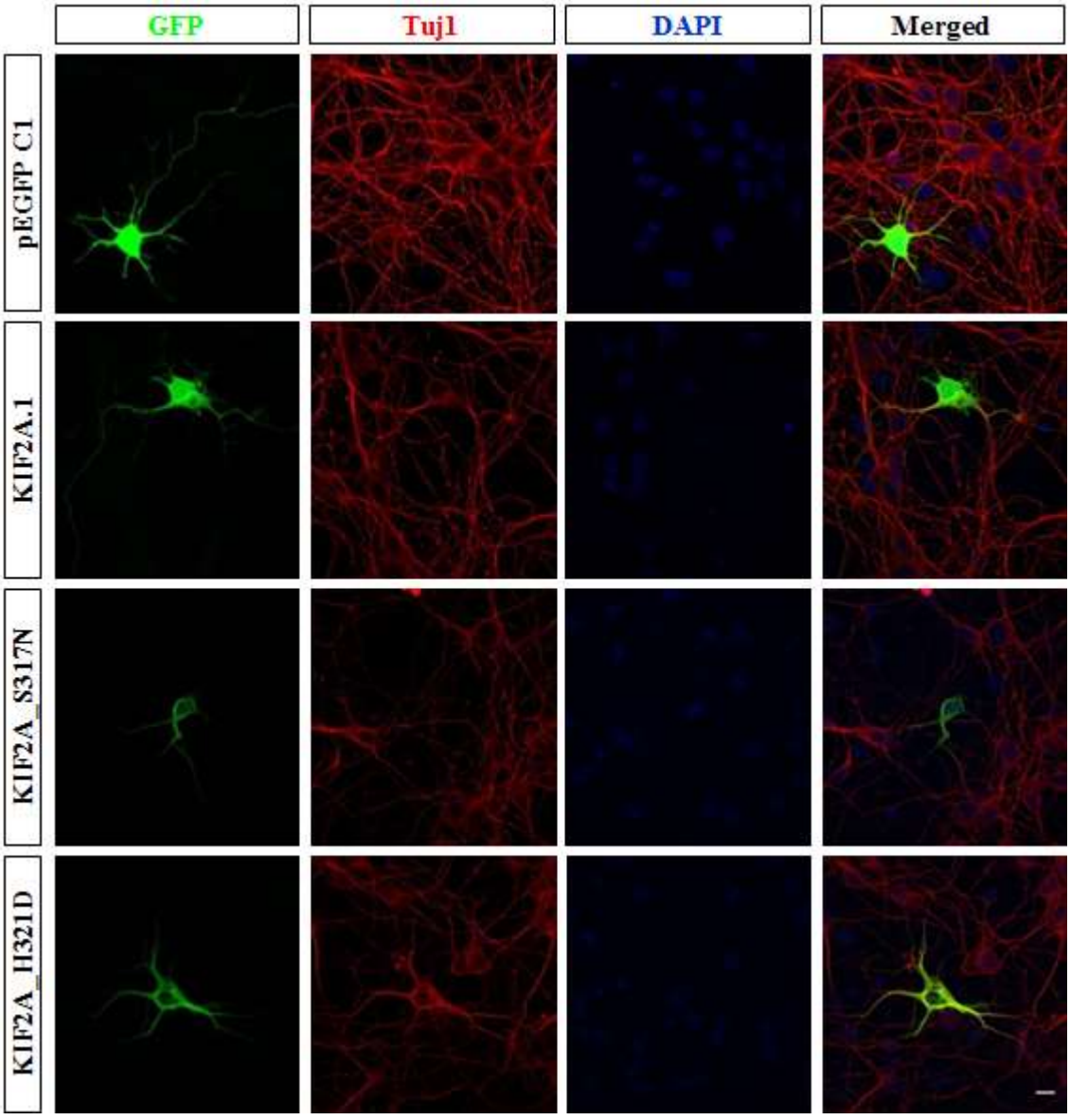

Figure 4.11: Immunofluorescence staining of KIF2A-GFP (green), Tuj1 (red) and DNA (blue) in E18 neurons that were transfected with pEGFP_C1 or KIF2A mutants (KIF2A_S317N, KIF2A_H321D) separately. Mutant KIF2A's localized only to the cytoplasm. Scale bar, 10µm.

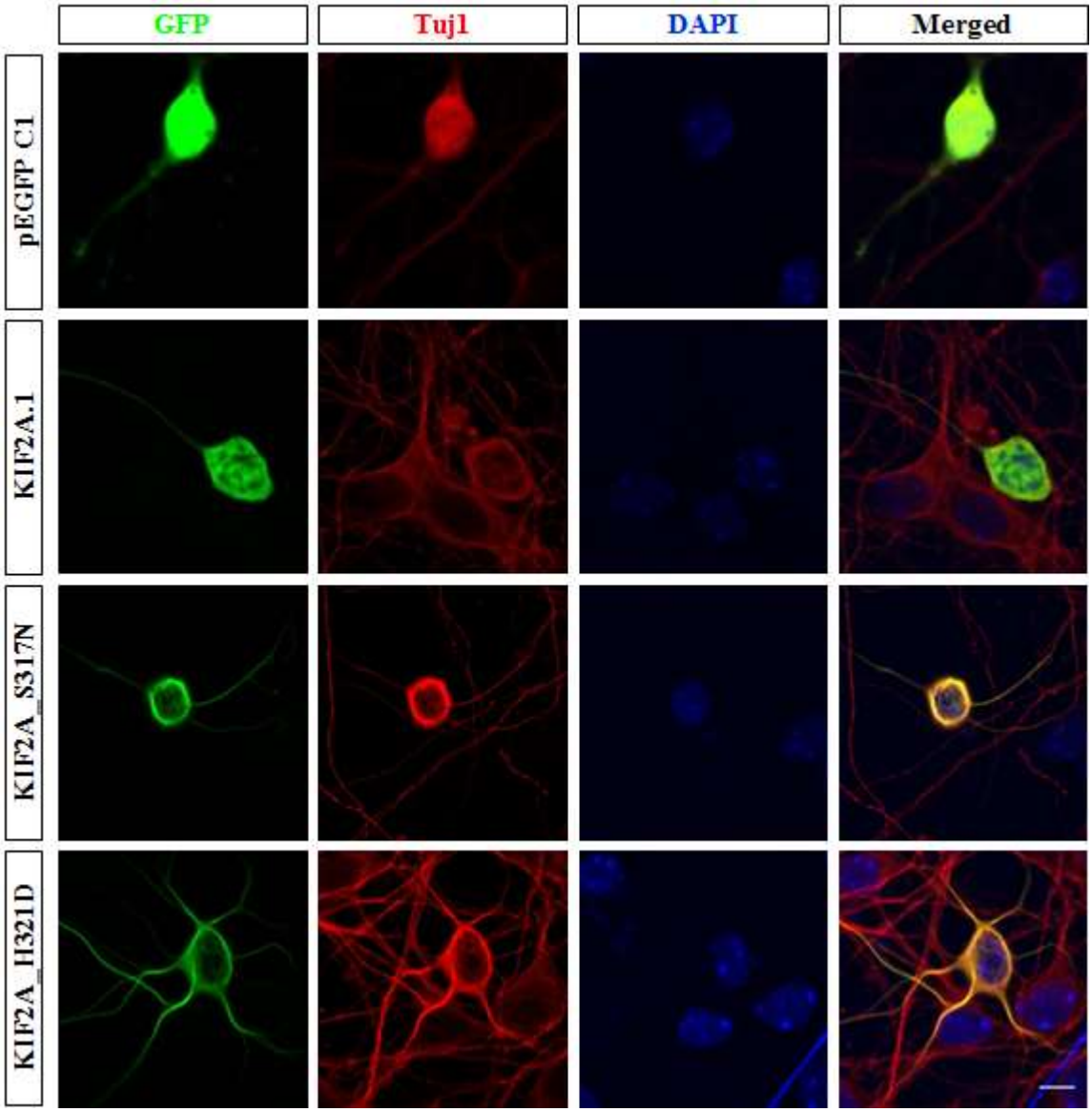

Figure 4.12: Higher magnification image of Figure 4.11 where the cage like structures can be clearly observed in KIF2A_S317N and KIF2A_H321D in E18 neurons. Scale bar, 10μm.

4.6 Co-localization of KIF2A_S317N and KIF2A_H321D with stable and dynamic microtubules

Since KIF2A has a role in microtubule depolymerization, we wanted to determine if KIF2A mutants co-localized with stable and/or dynamic microtubules. Mutants were overexpressed in E14 primary neuronal cultures by transfection with Lipofectamine2000® reagent. After fixation, they were stained with GFP and markers of dynamic (tyrosinated tubulin) and stable (detyrosinated tubulin) microtubules. Results demonstrated that, KIF2A mutants are interacting with mainly dynamic microtubules (Figure 4.13 and 4.14) and at least a subpopulation co-localizes with stable microtubules (Figure 4.15 and 4.16).

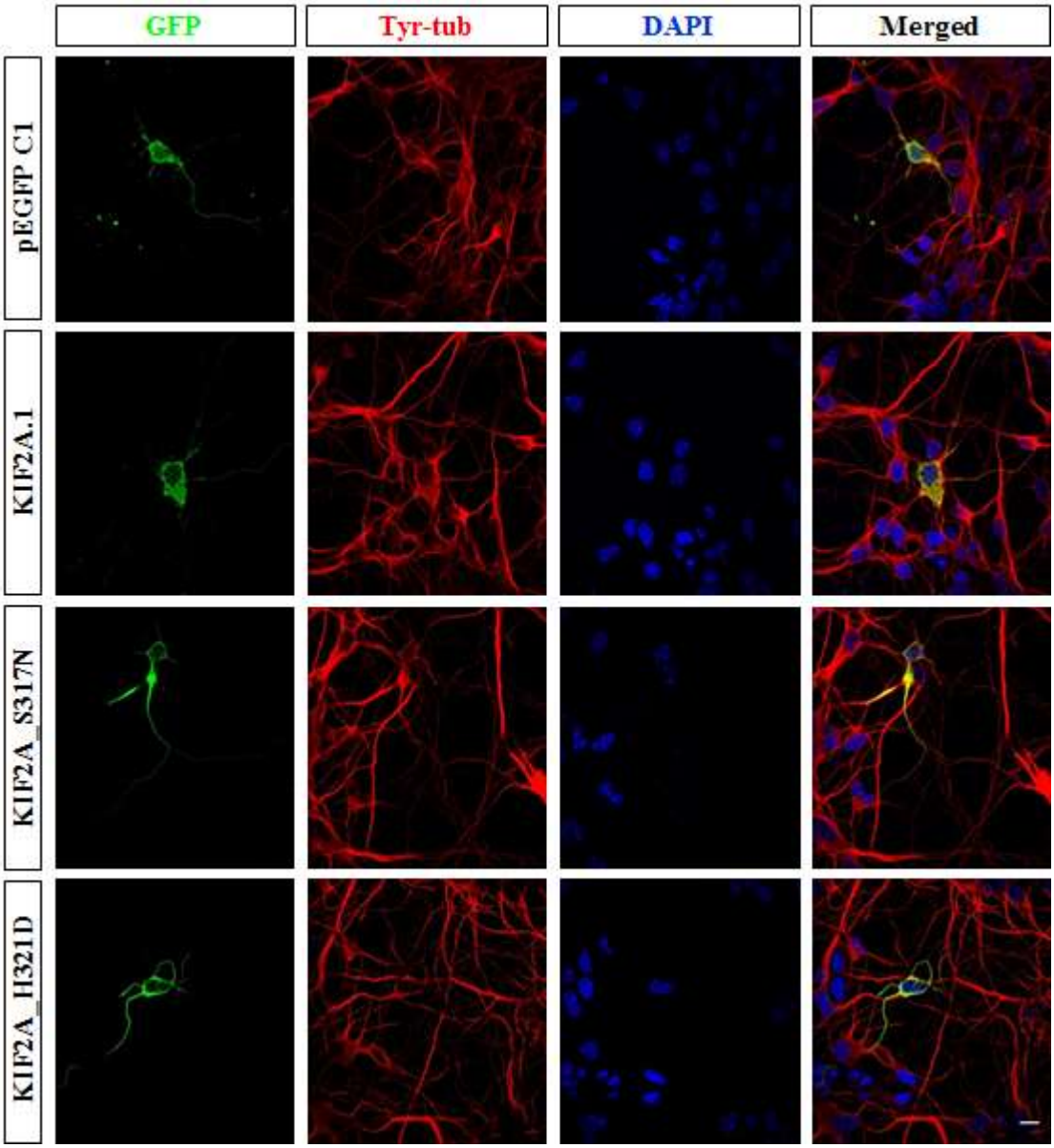

Figure 4.13: Immunofluorescence staining of KIF2A-GFP (green), dynamic microtubules (red) and DNA (blue) in E14 primary neurons that were transfected with pEGFP_C1 or KIF2A mutants (KIF2A_S317N and KIF2A_H321D) separately. Scale bar, 10μm.

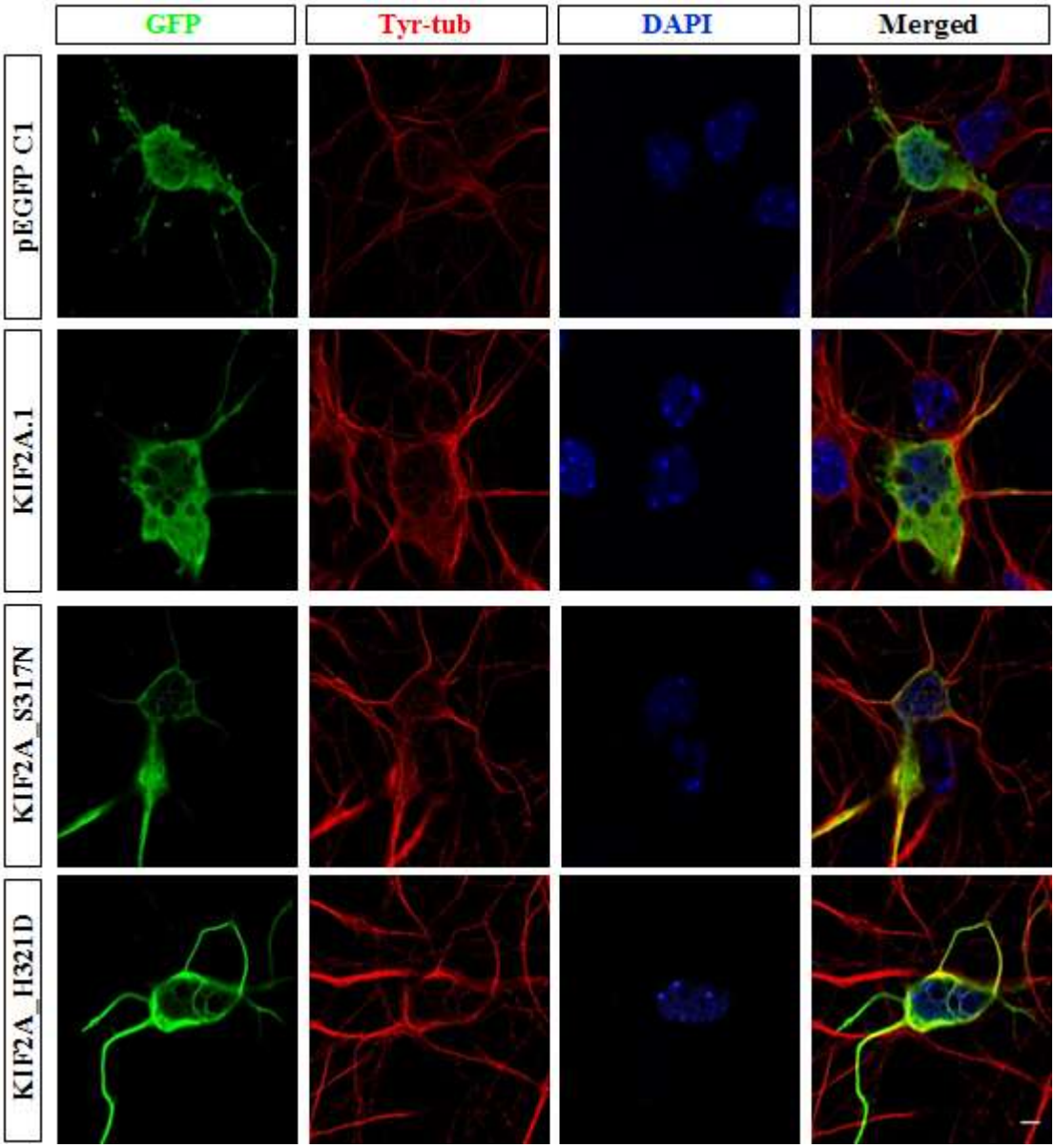

Figure 4.14: Higher magnification image of Figure 4.13. Scale bar, 10µm.

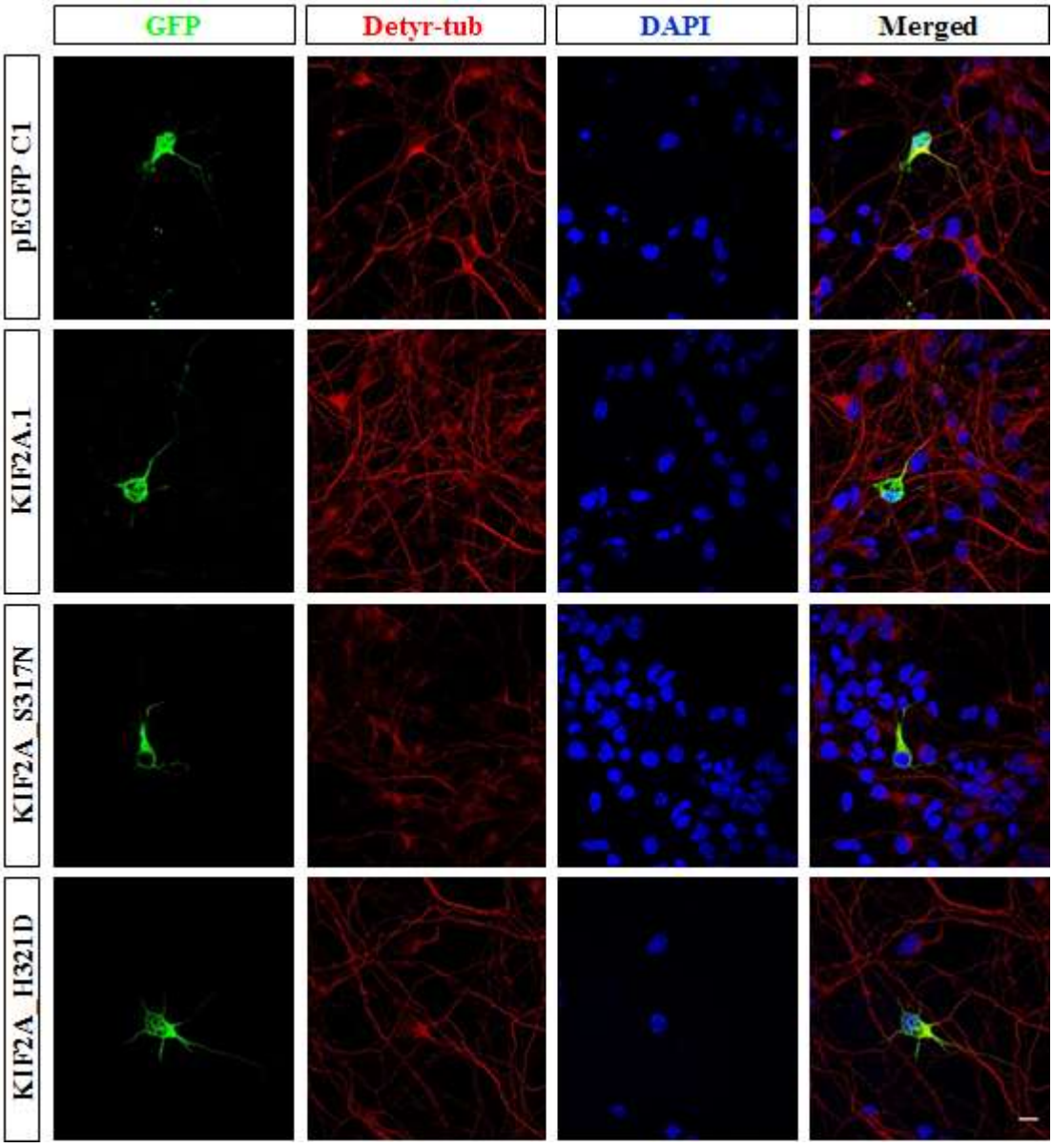

Figure 4.15: Immunofluorescence staining of KIF2A-GFP (green), stable microtubules (red) and DNA (blue) in E14 primary neurons that were transfected with pEGFP_C1 or KIF2A mutants (KIF2A_S317N and KIF2A_H321D) separately. Scale bar, 10μm.

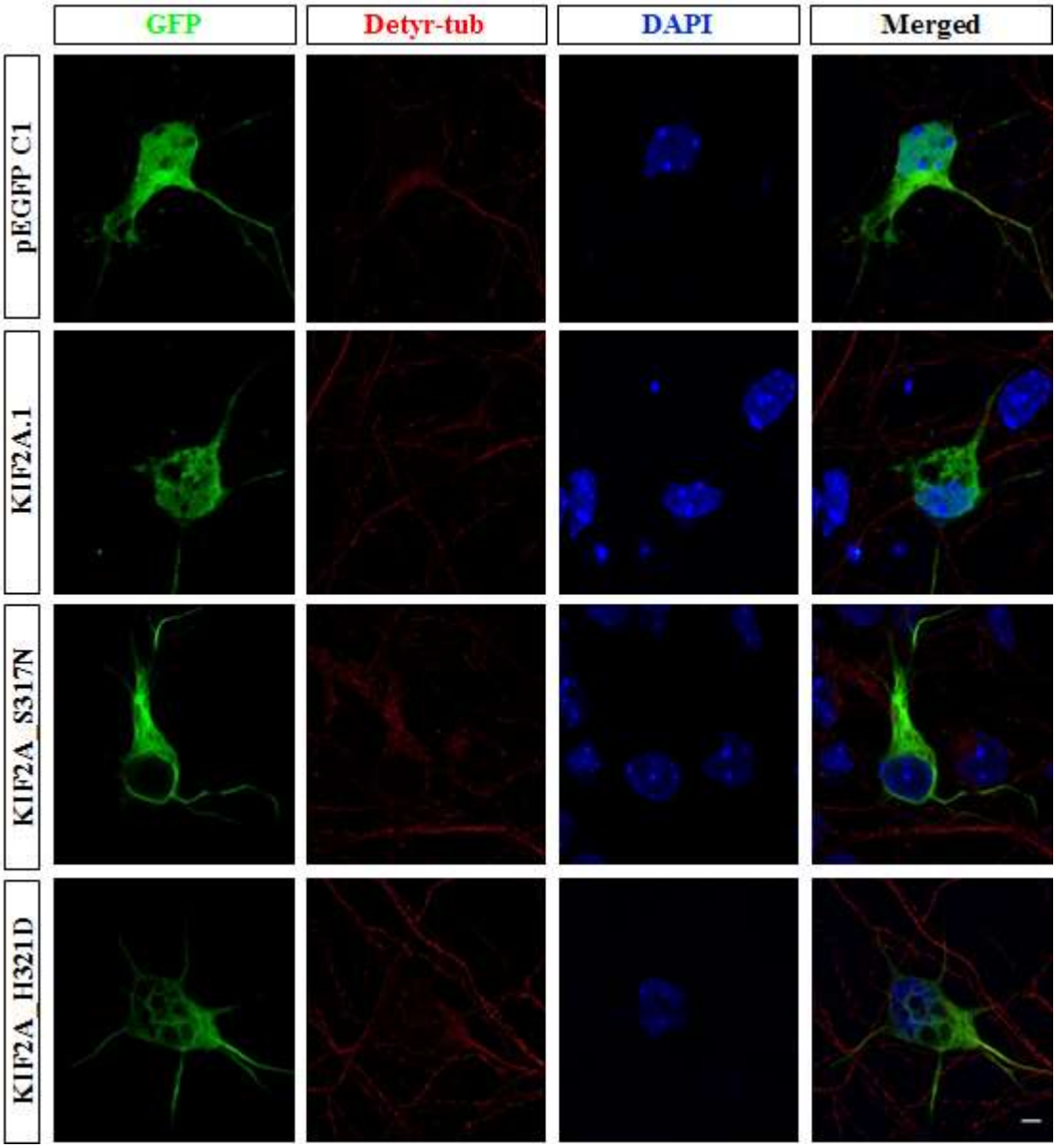

Figure 4.16: Higher magnification image of Figure 4.15. Scale bar, 10μm.

4.7 Effect of KIF2A_S317N and KIF2A_H321D on organelle trafficking

We found that different KIF2A isoforms' expression does not change the mitochondrial localization. Next, the effect of KIF2A mutants on organelle trafficking was observed. mCherry-TOMM20-N-10 construct was co-transfected with KIF2A mutants that were cloned into pEGFP_C1 backbone vector in E14 primary neurons. After cells were co-transfected, they were fixed with 4% PFA and stained only with GFP since endogenous mCherry signal was very high. GFP antibody used to detect the transfected cells. Immunofluorescence results demonstrated that mitochondria localized mainly to the cytoplasm and also to the apical dendrites of neurons that were transfected with either of KIF2A mutants (Figure 4.17). Interestingly, mitochondrial puncta-like structures were observed on the neurons that were transfected with either KIF2A mutants (Figure 4.18 A, white arrows). For, neurons that were transfected with KIF2A.1, KIF2A_S317N and KIF2A_H321D; GFP positive cells that have with or without puncta-like mitochondrial structures were counted under confocal microscope and graph was plotted by normalizing the cells to 100. Results demonstrated that puncta-like mitochondrial structures were higher in KIF2A mutants than KIF2A.1 (Figure 4.18 B). Overall, these results demonstrated that KIF2A mutants may affect the mitochondrial biogenesis and/or mitochondrial trafficking.

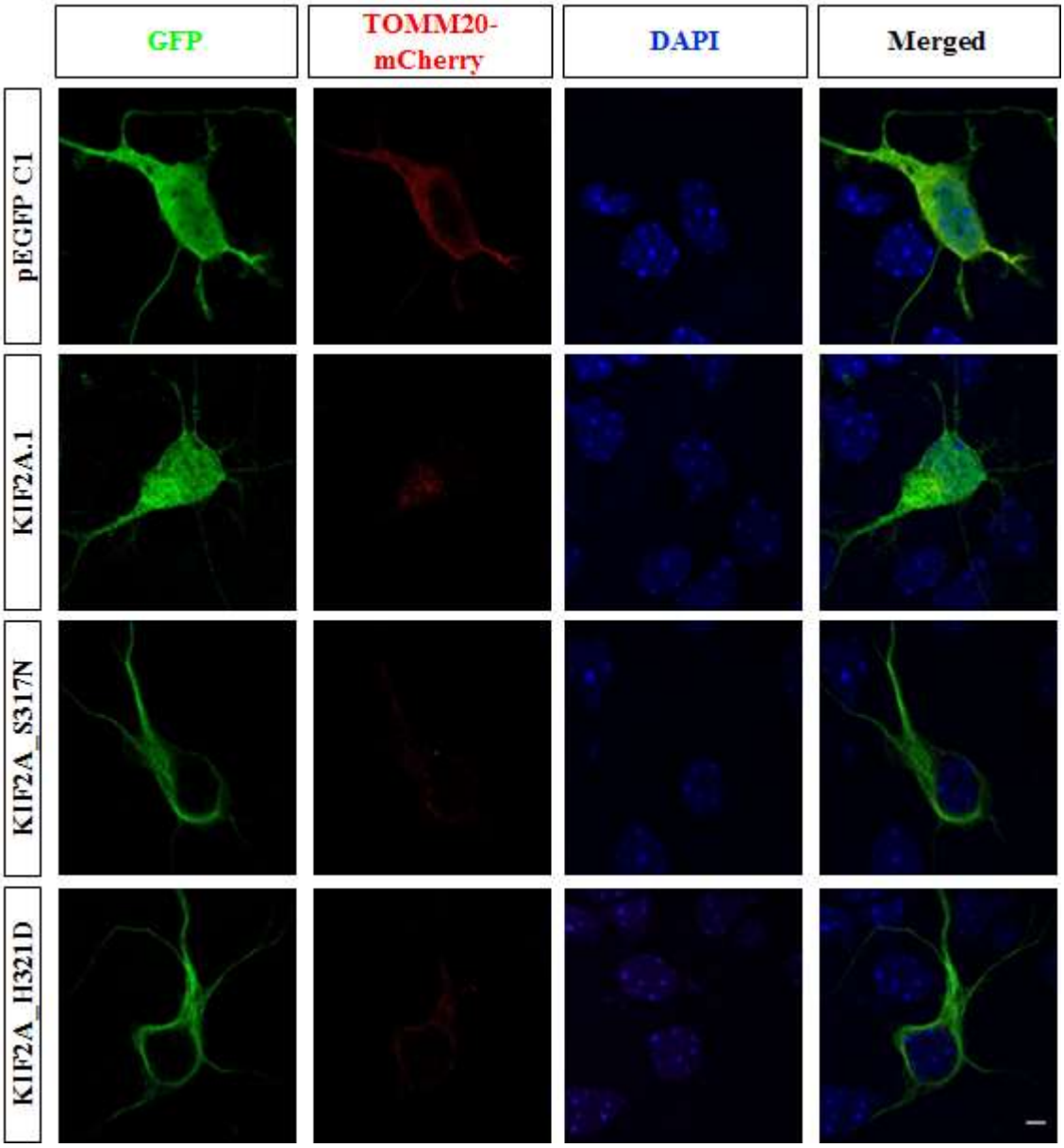

Figure 4.17: Immunofluorescence staining of KIF2A-GFP (green), mitochondria (red) and DNA (blue) in E14 neurons that were transfected with pEGFP_C1 or KIF2A mutants (KIF2A_S317N, KIF2A_H321D) separately. Scale bar, 10μm.

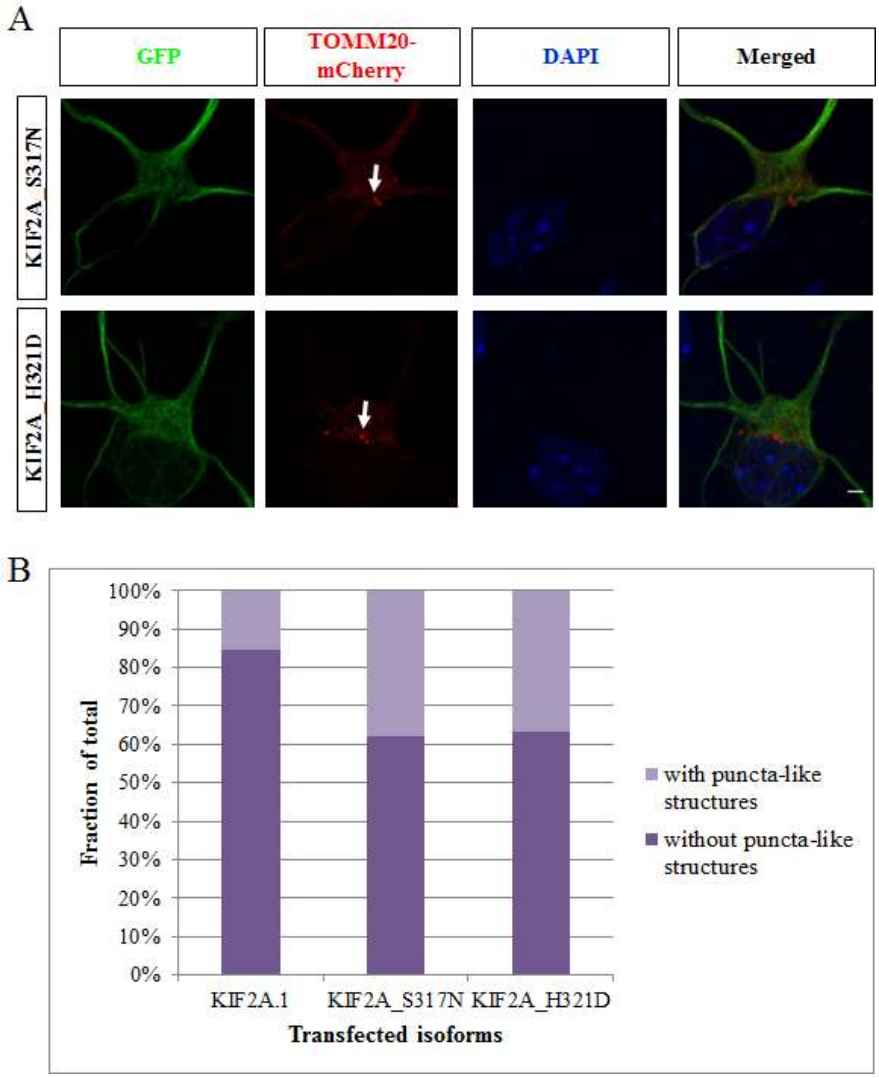

Figure 4.18: A. Immunofluorescence staining of KIF2A-GFP (green), mitochondria (red) and DNA (blue) in E14 neurons that were transfected with KIF2A mutants (KIF2A_S317N, KIF2A_H321D), separately. Scale bar, 10µm. Arrows show the mitochondrial puncta. **B.** Fraction of mitochondrial with or without puncta-like structures in neurons (normalized to 100) that are transfected with KIF2A.1, KIF2A_S317N and KIF2A_H321D (n=26, 42, 98 respectively).

4.8 Cloning of *BirA*-Kif2a* constructs

In order find proteins that KIF2A interacts with, BioID method was performed. BioID is a method which screens protein by expressing biotin ligase fusion of KIF2A in cells, followed by streptavidin bead isolation of biotinylated proteins and mass spectrometric characterization (Figure 4.19). Using this method, differential protein binding partners of KIF2A isoforms (KIF2A.1 and KIF2A.2), and one mutant (KIF2A_H321D) were identified. To use this method, first of all, KIF2A cDNAs were cloned into pcDNA3.1(-) mycBirA (BirA*) by using PCR based method. This vector allowed the expression of KIF2A as a mycBirA* fusion protein. The KIF2A's were amplified from pEGFP_C1 vector by PCR. After restriction enzyme digestion and ligation with BirA* vector, constructs were transformed into chemically competent DH5α *E.coli*. After colony selection and miniprep; digestion was carried out, samples were run on 1% agarose gel searching for an insert (Figure 4.20 A, B). Samples were sent to direct sequencing for verification.

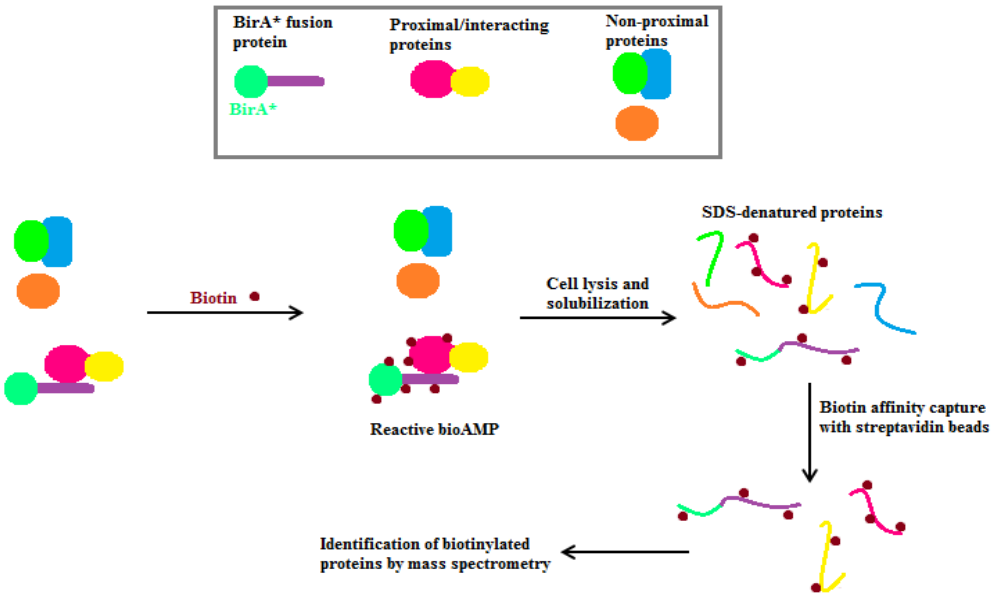

Figure 4.19: Schematic outline of BioID method (Adapted from [44]).

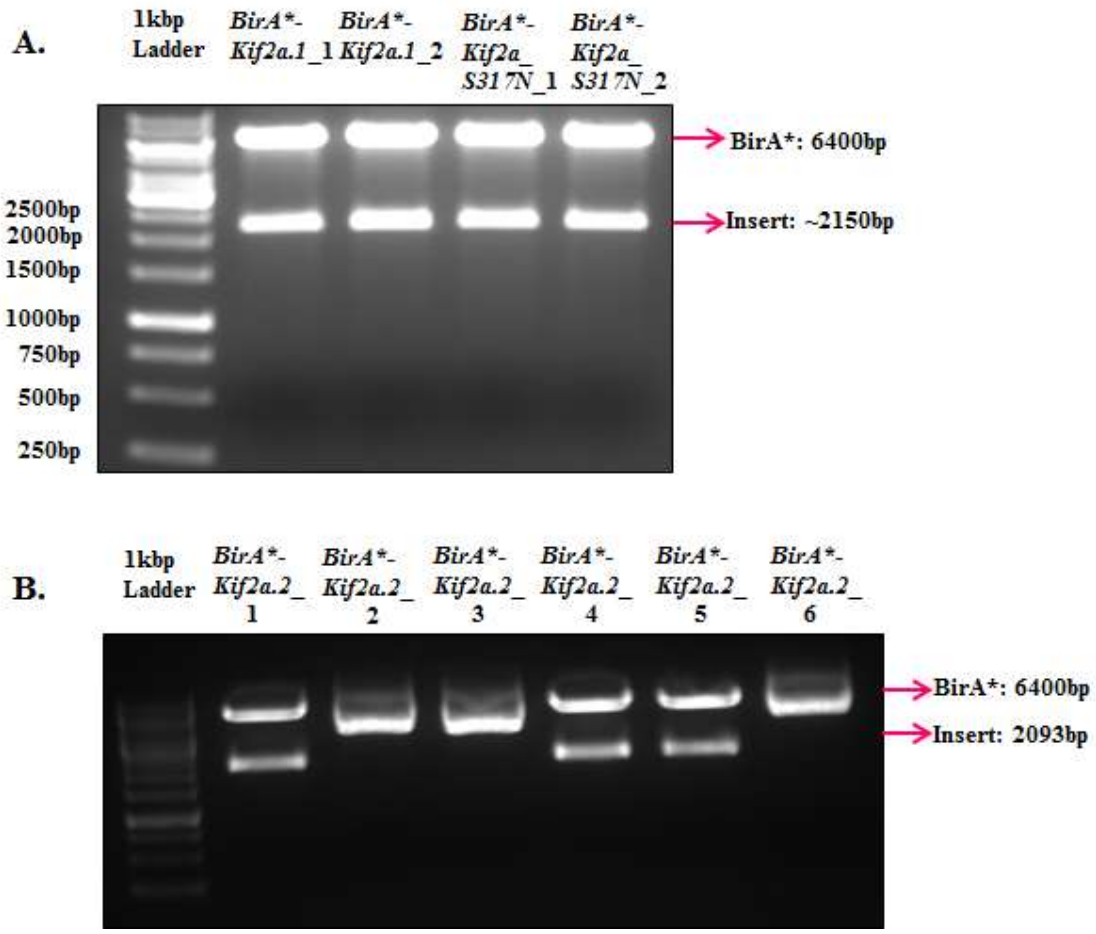

Figure 4.20: *BirA*-Kif2a* constructs were verified by diagnostic digestion. Agarose gel electrophoresis results after diagnostic digestion **A.** *BirA*-Kif2a.1* and *BirA*-Kif2a_H321D* and **B.** *BirA*-Kif2a.2*. Lanes 1, 4 and 5 had the correct insert.

4.9 Co-localization and expression of BirA*-KIF2A constructs by western blot and immunofluorescence

Before starting BioID experiments, *BirA*-Kif2a* constructs (*BirA*-Kif2a.1, BirA*-Kif2a.2, BirA*-Kif2a_H321D*) were transfected into Neuro2A cells to verify both expression of constructs and co-localization with biotin in Neuro2A cells. One day after transfection, biotin was added onto cells so that BirA*-KIF2A constructs could biotinylated proximal proteins. One day after biotinylation, cells were fixed and stained with myc (green) and Streptavidin-Alexa 594 which was used to detect biotin (red). As expected, transfected cells were positive with biotin and myc (Figure 4.21).

Next, after transfection and biotinylation, cells were collected and western blot was done to confirm the success of the transfection (Figure 4.22). First, membrane was incubated with α-Histone H3 antibody to see whether proteins were loaded equally (Figure 4.22 bottom panel). Then the blot was stripped with α-myc primary antibody to see whether BirA*-KIF2A overexpression was successful, since BirA* vector has a myc tag (Figure 4.22 top panel). Western blot with α-myc antibody showed that the BirA*-KIF2A constructs were transfected successfully. In non-transfected cells, no band was seen in the α-myc blot. Moreover, in BirA* transfected cells, a band around 35 kDa was observed since BirA*-myc tag protein is 36 kDa. Finally, blot was stripped with α-biotin antibody to verify the biotinylation (Figure 4.22 middle panel).

Both immunofluorescence and western blot experiment showed that, the transfection with different *BirA*-Kif2a* were expressed successfully in Neuro2A cells and all constructs co-localized with biotin.

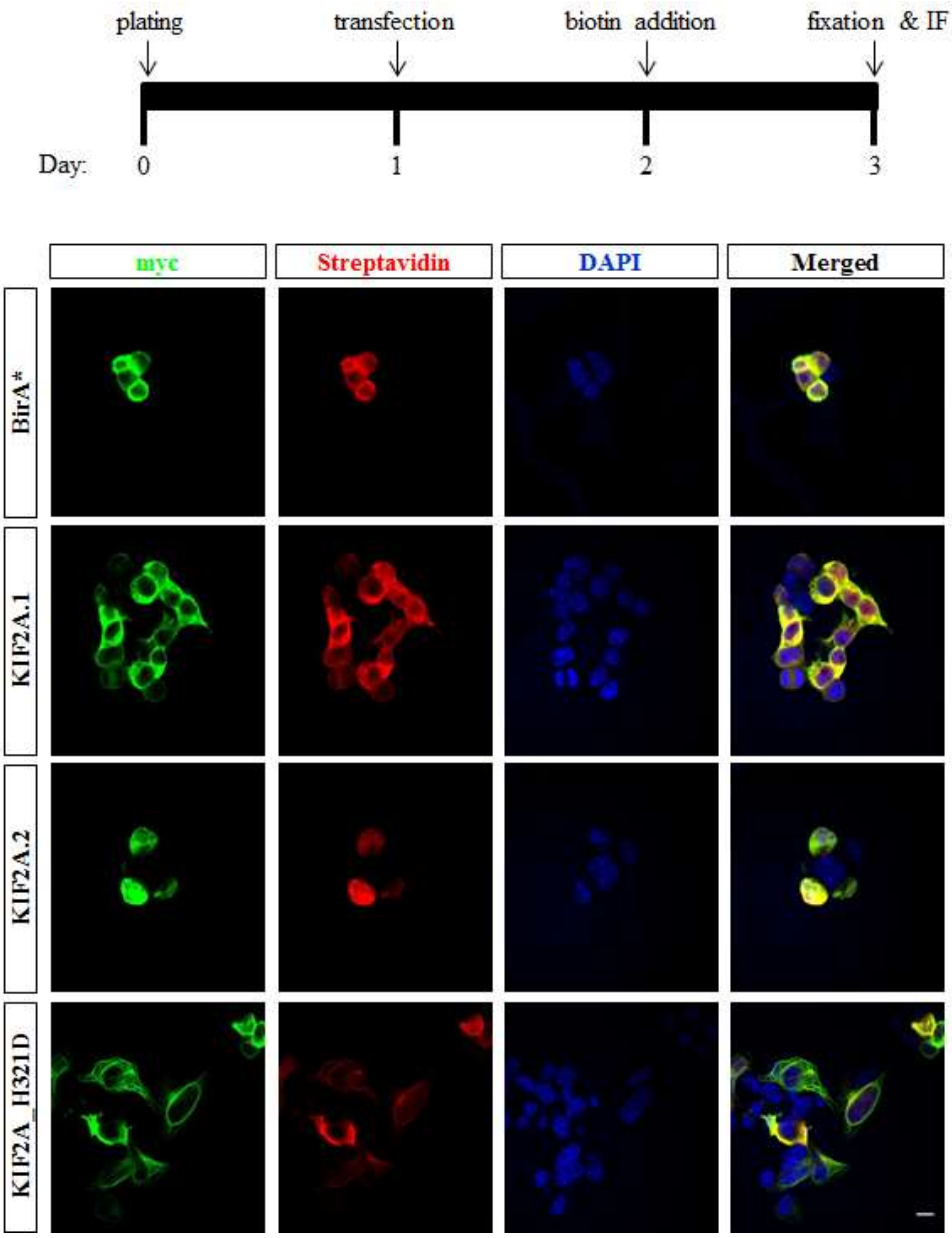

Figure 4.21: Immunofluorescence staining of KIF2A (green), biotin (red) and DNA (blue) in Neuro2A cells that were transfected with *BirA** only, *BirA*-Kif2a.1*, *BirA*-Kif2a.2* and *BirA*-Kif2a_H321D* separately. Scale bar, 10µm.

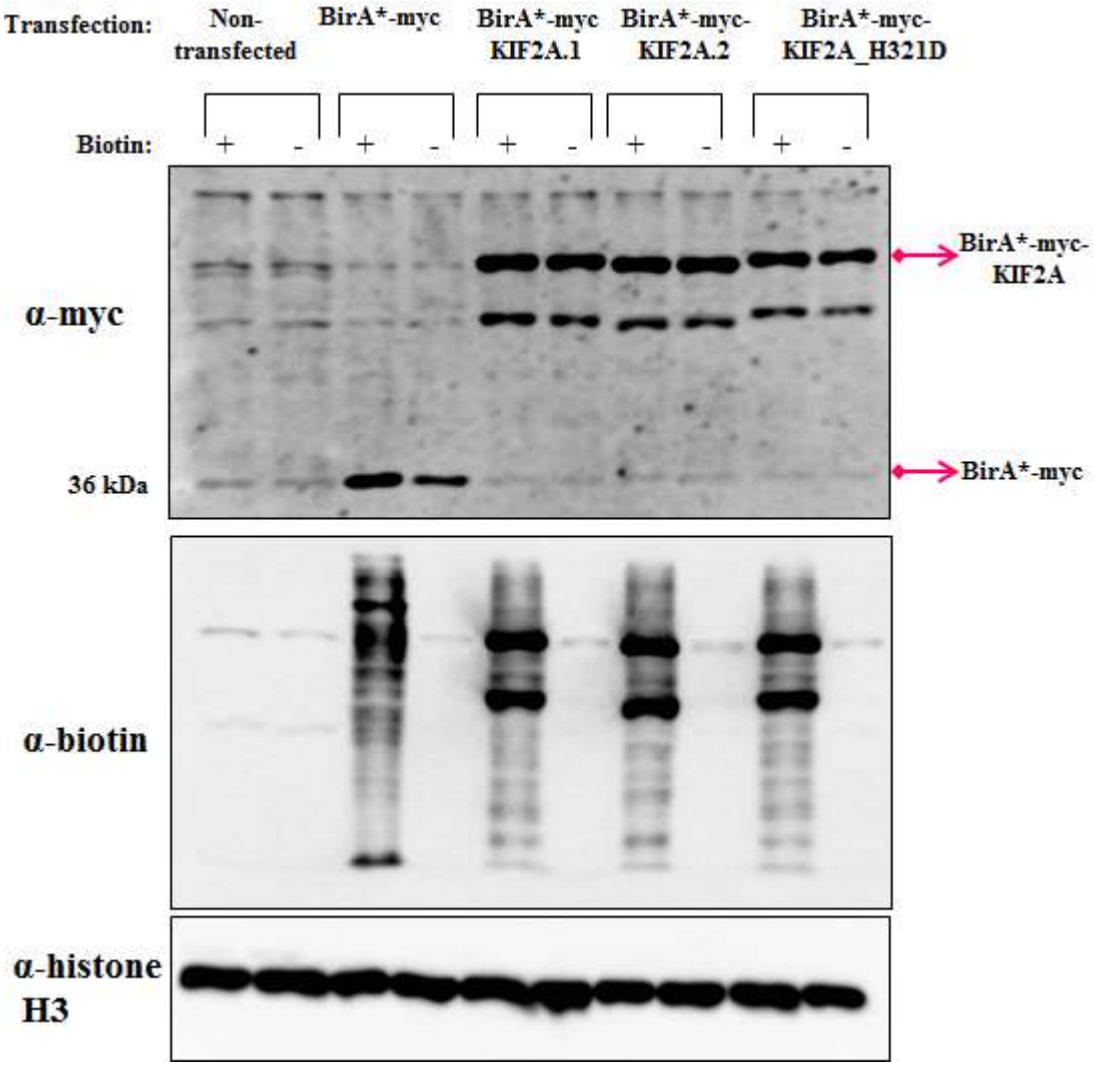

Figure 4.22: Western blot result showed that Neuro2A cells overexpressed BirA*-KIF2A successfully. Non-transfected and BirA* transfected lanes were negative controls. Top panel: western blot with α-myc showed that success of the transfection. Middle panel: western blot with α-biotin showed the biotinylation was successful. Bottom panel: western blot with α-Histone H3 was done as a loading control.

4.10 Pull-down of biotinylated BirA*-KIF2A constructs by streptavidin beads

Biotinylated proteins were pulled down with streptavidin beads. Neuro2A cells were transfected with *BirA**, *Bira*-Kif2a.1*, *BirA*-Kif2a.2* or *BirA*-Kif2a_H321D* and biotin was added next day. One day after biotinylation cells were lysed, 50 µl of input was saved and 600 µl lysate for each condition was added onto 60 µl streptavidin beads and mixed overnight. Next day, beads were washed with wash buffers and 30 µl SDS sample buffer was added onto beads, 10 µl of SDS sample buffer was added on 10 µl of input and they were boiled at 95^{o}C for 5 minutes and then loaded on SDS-gel. After SDS-PAGE, wet transfer was done and membranes were incubated with α-biotin antibody (Figure 4.23). The input blot confirmed that the proteins were biotinylated and the pull-down blot confirmed that the biotinylated proteins were pulled down successfully by using streptavidin beads. In both pull-down and input blots, different banding patterns were observed between BirA*-KIF2A.1 and BirA*-KIF2A.2 isoforms. The banding pattern between BirA*-KIF2A.1 and BirA*-KIF2A_H321D was nearly the same. Input blot was stripped with α-beta actin antibody to confirm that proteins were loaded equally on the gel.

Moreover, pull-down samples and inputs were loaded onto SDS-polyacrylamide gel and silver staining was done to observe the bands (Figure 4.24). At the bottom of the gel, there was a huge band in pull-down lanes. Streptavidin is a tetrameric protein which has a molecular weight around 52 kDa so its monomer is around 13 kDa. When streptavidin beads were boiled with SDS sample buffer, streptavidin monomers leaked into the buffer.

To optimize the bead concentration, different amount of beads were used to pull down the biotinylated proteins (Figure 4.25). Neuro2A cells were either not transfected or transfected with *BirA** and biotinylated the next day. One day after biotinylation, cells were collected and 50µl was saved as an input and rest was divided into four. For each condition 200µl of input was added into 5µl, 10µl, 25µl and 50µl streptavidin beads and biotinylated proteins were pulled-down with streptavidin beads. 30µl of SDS sample buffer was added and boiled at 95^{o}C for 5 minutes. Western blot was done by using α-biotin antibody (Figure 4.25A). When the amount of the beads increased the band intensity decreased for both non-transfected and *BirA** transfected lanes, which means 5µl of streptavidin beads was enough to pull down 200µl of biotinylated proteins. Silver staining was done to confirm that there was a minimum amount streptavidin monomer in the lane that had a 5 µl bead (Figure 4.25B). Thus, in large scale BioID experiments, 5 µl of streptavidin beads was used per 200µl lysate.

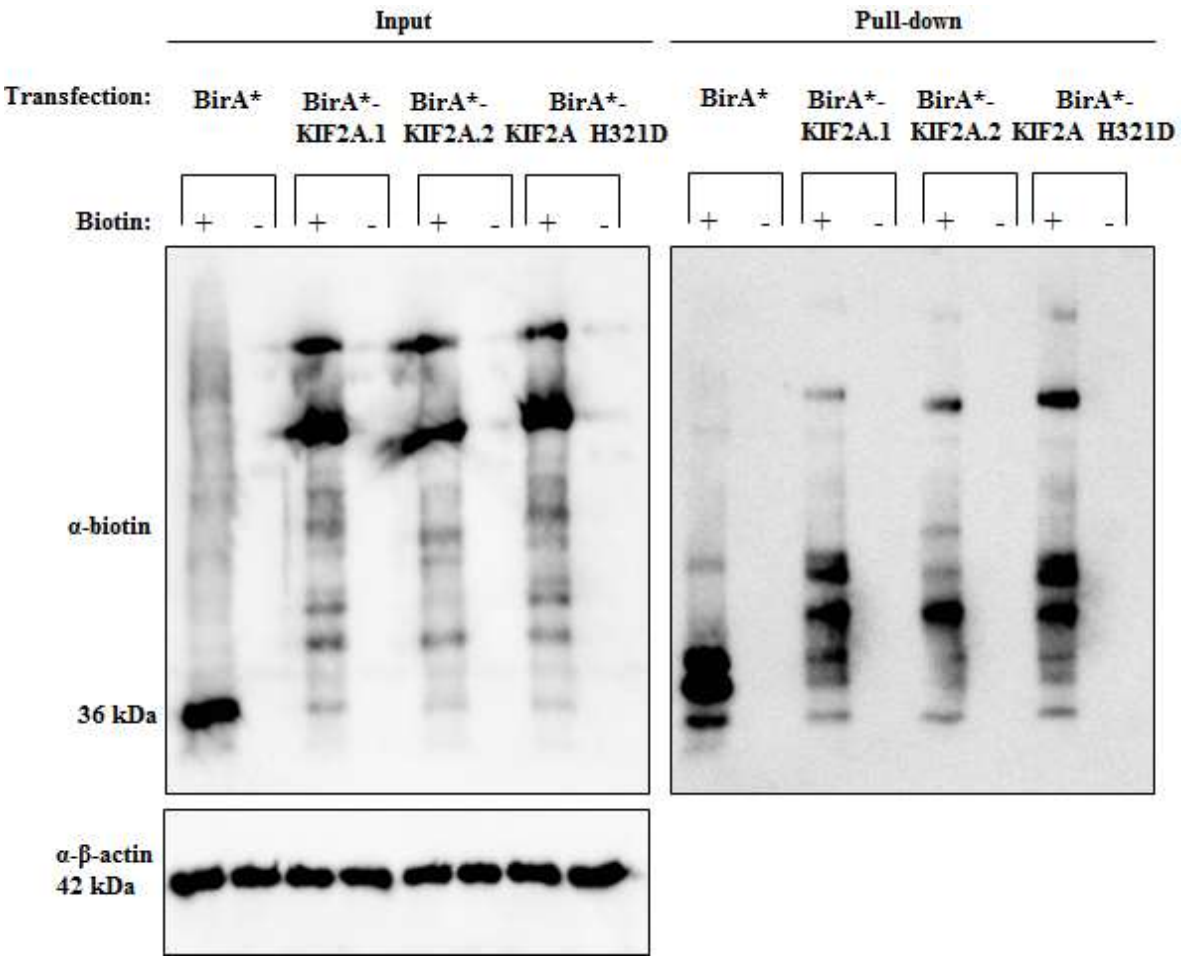

Figure 4.23: Western blot against biotin antibody for both input and pull-down. Pull-down blot confirm the pull-down and input blot confirm that the proteins were biotinylated. β-actin was used as a loading control.

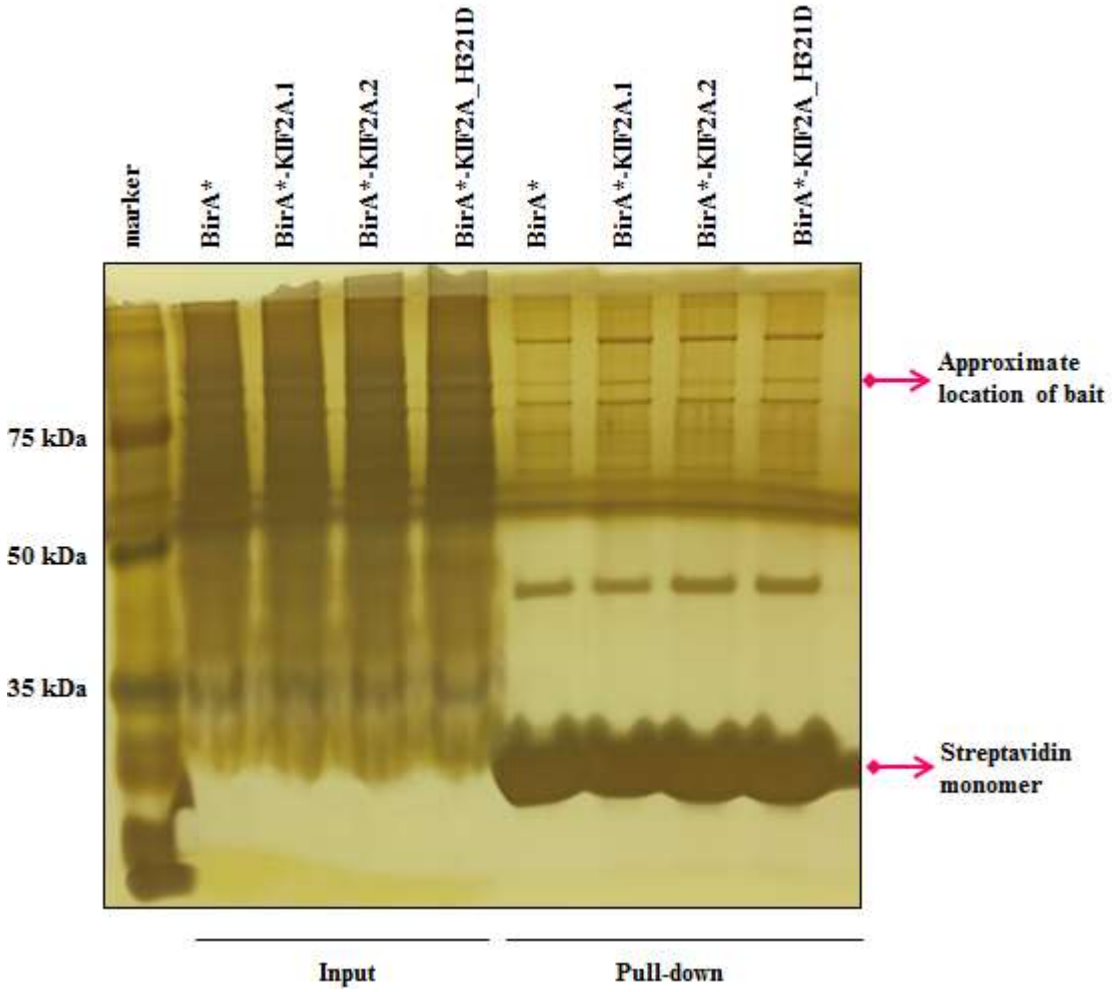

Figure 4.24: Silver staining results for both input and pull-down of different BirA*-KIF2A constructs. Intense band around 15 kDa in pull-down samples were streptavidin monomers.

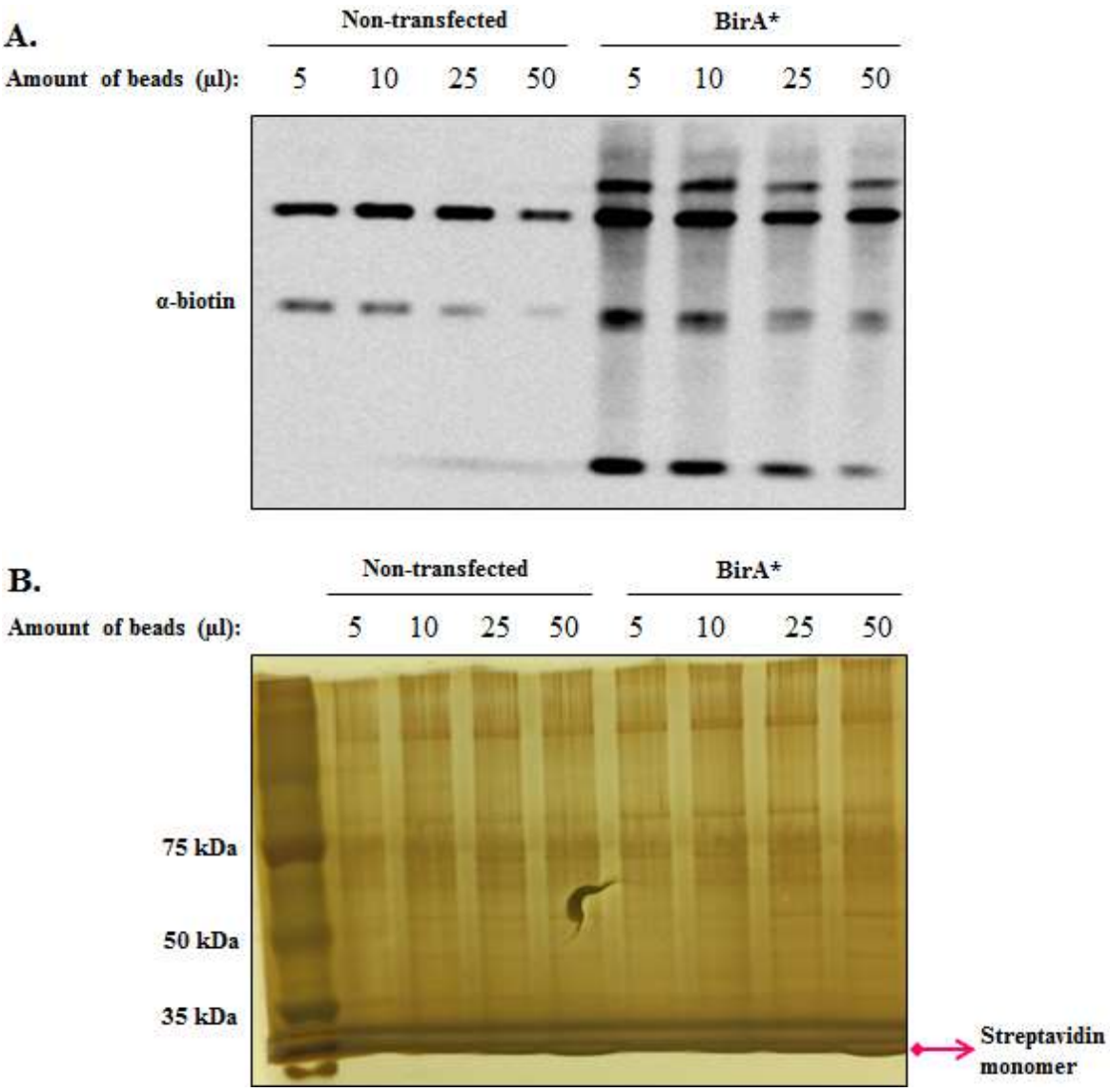

Figure 4.25: Bead amounts were optimized by using different amount of beads in pull down. **A.** Western blot against biotin showed 5µl of streptavidin bead was enough to pull-down the biotinylated proteins. **B.** Silver staining showed 5µl of streptavidin bead gave minimum amount of streptavidin monomer.

4.11 Identification of binding partners of KIF2A by Mass spectrometry

After confirming both the expression and the pull-down of different BirA*-KIF2A constructs, large scale pull-down was done for BioID experiments. For each condition (non-transfection, BirA*, BirA*-KIF2A.1, BirA*-Kif2A.2 and BirA*-KIF2A_H321D) five 10 cm plates were prepared and Neuro2A cells were transfected with these constructs. One day after, they were biotinylated. One day after biotinylation, they were lysed and mixed with 50µl streptavidin beads. Input and beads were incubated overnight and the next day they were washed and eluted in 250µl ammonium bicarbonate. After elution they were sent to mass spectrometry to find the interaction partners of KIF2A.1, KIF2A.2 and KIF2A_H321D.

Chapter 5

DISCUSSION

This study identifies differential roles of *Kif2a* mRNA isoforms and mutants and reveals differential protein binding partners of KIF2A. The findings are important because KIF2A has a role in inhibition of axonal branching by depolymerizing the microtubules and mutations on *Kif2a* causes cortical malformations in humans [9], [10], [12].

nElavl family (Elavl2, Elavl3 and Elavl4) are RNA binding proteins that regulate alternative splicing of several neuronal pre-mRNAs, by binding to specific intronic sequences[1], [8]. One of the targets of nElavl is *Kinesin superfamily protein 2a (Kif2a)* pre-mRNA, encoded by a gene which has roles in axonal morphogenesis. Ince-Dunn *et al.* demonstrated that *Elavl3/4* knockout in mice disrupts *Kif2a* alternative splicing at exon 18 and consequently affects isoform abundance. Binding of nELAVL on U-rich intronic sequences flanking exon 18 enhances the generation of KIF2A.1 isoform which includes alternative exon 18 and inhibits the formation of KIF2A.2 that lacks exon 18 [8]. I found that nELAVL protein expression is developmentally controlled; expression decreases at postnatal day 21 and later developmental stages in mice. Interestingly, quantitative PCR analysis show that alternative splicing of *Kif2a* exon 18 does not change during development. There is no significant difference between *Kif2a.1* and *Kif2a.2* mRNA compositions when compare with different developmental points. Even though nELAVL expression decreased, *Kif2a* mRNA stability increased. nELAVL binds not only intronic sequence flanking to exon 18, but also 3'UTR of the pre-mRNA which may cause the

destabilization of *Kif2a* pre-mRNA. Alternatively, other factors that are currently unknown influence the alternative splicing of *Kif2a* gene.

Three *Kif2a* isoforms were identified which are *Kif2a.1*, *Kif2a.2* and *Kif2a.3.* Localization of these three isoforms was determined and my results showed that they all localize to both nucleus and cytoplasm in both Neuro2A cell line and primary neuronal cultures. Thus, there is no difference between localization patterns of the isoforms.

MTs are one of the main elements that forms cytoskeleton and regulation of depolymerization-polymerization equilibrium of the MTs are very crucial in order to preserve the cell's shape. Since KIF2A has a role in microtubule depolymerization [12], and KIF2A isoforms co-localize with Tuj1 which is a neuronal microtubule marker, I wanted to decide whether different KIF2A isoforms co-localize with stable and/or dynamic MTs. Dynamic MTs are found on cell body, axon, primary and apical dendrites and the growth cone of the neurons. Stable MTs are found on cell body, primary dendrites and axon of the neurons. All KIF2A isoforms that interact with MTs co-localize mainly with dynamic microtubules and at least a subpopulation is interacting with stable microtubules. Thus, there is no difference between the co-localization of isoforms with MTs.

Rogers *et al.* showed that cytoskeleton-associated motor proteins regulates the organelle trafficking in eukaryotic cells [43]. MT depolymerization role of KIF2A may also have role in the organelle trafficking. Mitochondrion is selected as a target organelle and it is found in cell body and apical dendrite of the neurons. Different KIF2A isoforms does not change the mitochondria trafficking. Neurons that express one of the three KIF2A isoforms have mitochondria in their cell bodies and apical dendrites.

Poirier *et al.* identified two different missense point mutations which cause cortical malformations in humans. These dominant negative point mutations were found on motor domain of KIF2A and the mutated amino acid residues are conserved in mice [9]. I generated humanized mutations in Kif2a cDNA and overexpressed them in N2A cell line and primary cortical neurons. Localization of KIF2A changed when mutants were expressed in both Neuro2A cells and primary neurons. Instead of localizing to both nucleus and cytoplasm, these two KIF2A mutants localized only to cytoplasm and they were forming cage like structures. The reason why KIF2A is absent in nucleus may be because all the mutant KIF2A's bind to MTs and they cannot free from MTs so that there is no free KIF2A in the cell. I wanted to know whether these cage-like structures are dynamic and/or stable MTs. I found that two KIF2A mutants co-localize with both mainly dynamic MTs and at least a subpopulation co-localize with stable MTs, so these point mutations does not affect the co-localization with either type of the MTs.

To look the effects of KIF2A in organelle trafficking co-transfection of GFP-fused KIF2A and mCherry-TOMM20 which is a mitochondrial marker was done and the localization of the mitochondria was observed under confocal microscope. Mitochondrion trafficking does not change in the mutants; mitochondria are localized in the cell body and the apical dendrite like in the wild type. Interestingly, I observed puncta-like mitochondrial structures on the neurons that were transfected with either KIF2A mutants. Normally, mitochondria are organelles that fuse and divide dynamically [45]. I hypothesized that these puncta-like mitochondrial structures may be the mitochondria that were failed to divide after fusion. Results showed that puncta-like mitochondrial structures were higher in KIF2A mutants than KIF2A.1 which may affect mitochondrial biogenesis.

In this study, BioID method was performed to identify differential protein binding partners for different KIF2A protein isoforms. Biotin ligase fusion of KIF2A was expressed in Neuro2A cells and biotinylated proteins that interact with KIF2A were isolated by streptavidin beads and then analyzed by mass spectrometry.

Before starting the BioID experiment, some of the parameters had to be confirmed. By using western blot and immunofluorescence success both biotinylation and transfection were confirmed. Western blot was done against anti-myc which showed transfection was successful since the BirA* vector has a myc tag and also blot was stripped with anti-biotin to show that biotinylation was successful. In the immunofluorescence cells were stained by using anti-myc to confirm that transfection was successful and we also used streptavidin-alexa to verify the biotinylation since biotin has an affinity to streptavidin. I also confirmed the pull-down by boiling the beads after pull-down and run the proteins on SDS-acrylamide gels and did a western blot against anti-biotin. I verified the pull-down in this experiment and also observed different banding patterns in KIF2A.2. In the KIF2A.1 and KIF2A_H321D, the banding patterns looked the same and there are two bands that were observed in these isoforms that were not observed in the KIF2A.2. I couldn't say what are these differences corresponds to but my BioID result is showing which proteins make this difference.

Future Directions

At the organismal level alternative splicing generates increased proteomic and phenotypic complexity. Our results demonstrating that protein isoforms of KIF2A differentially interact with protein binding partners supports the premise that alternative splicing mechanisms have the capacity to rewire protein interaction networks within the cell. In this study, effects of KIF2A isoforms and mutants on organelle trafficking and co-localization of KIF2A with MTs were observed. In future studies, protein interactions with candidate genes that identified with BioID screen will be confirmed. Looking for the BioID results, the differential binding partners of KIF2A isoforms and their roles in the cortical development can be investigated. Also, endogenous KIF2A will be knocked-down and shRNA resistant KIF2A isoforms will be expressed in the neurons look if there is an effect of the endogenous KIF2A on neuronal function. In addition to these, effects of KIF2A isoform and mutants on dendrite and axon development will be investigated since KIF2A controls axonal branching. Moreover, roles of KIF2A in cell cycle can also be analyzed because MTs has a major role in cytokinesis. Our results will shed light to understanding the molecular mechanisms by which the neuronal cytoskeleton is regulated and how it affects cortical development.

BIBLIOGRAPHY

[1] C. Colombrita, V. Silani, and A. Ratti, “ELAV proteins along evolution: Back to the nucleus?,” *Mol. Cell. Neurosci.*, vol. 56, pp. 447–455, 2013.

[2] F. Spitz and E. E. M. Furlong, “Transcription factors: from enhancer binding to developmental control,” *Nat. Rev. Genet.*, vol. 13, no. 9, pp. 613–626, 2012.

[3] K. D. Mansfield and J. D. Keene, “The ribonome: a dominant force in co-ordinating gene expression.,” *Biol. Cell*, vol. 101, no. 3, pp. 169–181, 2009.

[4] K. C. Martin and A. Ephrussi, “mRNA Localization : Gene Expression in the Spatial Dimension,” *Cell*, vol. 136, no. 4, pp. 1–21, 2010.

[5] B. J. Goldie and M. J. Cairns, “Post-transcriptional trafficking and regulation of neuronal gene expression,” *Mol. Neurobiol.*, vol. 45, no. 1, pp. 99–108, 2012.

[6] H. J. Okano and R. B. Darnell, “A hierarchy of Hu RNA binding proteins in developing and adult neurons.,” *J. Neurosci.*, vol. 17, no. 9, pp. 3024–3037, 1997.

[7] A. Szabo, J. Dalmau, G. Manley, M. Rosenfeld, E. Wong, J. Henson, J. B. Posner, and H. M. Furneaux, “HuD, a paraneoplastic encephalomyelitis antigen, contains RNA-binding domains and is homologous to Elav and sex-lethal,” *Cell*, vol. 67, no. 2, pp. 325–333, Oct. 1991.

[8] G. Ince-Dunn, H. J. Okano, K. B. Jensen, W. Y. Park, R. Zhong, J. Ule, A. Mele, J. J. Fak, C. Yang, C. Zhang, J. Yoo, M. Herre, H. Okano, J. L. Noebels, and R. B. Darnell, “Neuronal Elav-like (Hu) Proteins Regulate RNA Splicing and Abundance to Control Glutamate Levels and Neuronal Excitability,” *Neuron*, vol. 75, no. 6, pp. 1067–1079, 2012.

[9] K. Poirier, N. Lebrun, L. Broix, G. Tian, Y. Saillour, C. Boscheron, E. Parrini, S. Valence, B. Saint Pierre, M. Oger, D. Lacombe, D. Geneviève, E. Fontana, F. Darra, C. Cances, M. Barth, D. Bonneau, B. D. Bernadina, S. N’guyen, C. Gitiaux, P. Parent, V. des Portes, J. M. Pedespan, V. Legrez, L. Castelnau-Ptakine, P. Nitschke, T. Hieu, C. Masson, D. Zelenika, A. Andrieux, F. Francis, R. Guerrini, N. J. Cowan, N. Bahi-Buisson, and J. Chelly, “Mutations in TUBG1, DYNC1H1, KIF5C and KIF2A cause malformations of cortical development and microcephaly.,” *Nat. Genet.*, vol. 45, no. 6, pp. 639–47, 2013.

[10] N. Homma, Y. Takei, Y. Tanaka, T. Nakata, S. Terada, M. Kikkawa, Y. Noda, and N. Hirokawa, "Kinesin superfamily protein 2A (KIF2A) functions in suppression of collateral branch extension," *Cell*, vol. 114, no. 2, pp. 229–239, 2003.

[11] S. Niwa, "Kinesin superfamily proteins and the regulation of microtubule dynamics in morphogenesis," *Anat. Sci. Int.*, vol. 90, no. 1, pp. 1–6, 2014.

[12] M. Maor-Nof, N. Homma, C. Raanan, A. Nof, N. Hirokawa, and A. Yaron, "Axonal Pruning Is Actively Regulated by the Microtubule-Destabilizing Protein Kinesin Superfamily Protein 2A," *Cell Rep.*, vol. 3, no. 4, pp. 971–977, 2013.

[13] K. J. Roux, D. I. Kim, and B. Burke, "BioID: A screen for protein-protein interactions," *Curr. Protoc. Protein Sci.*, no. SUPPL.74, pp. 1–14, 2013.

[14] A. E. McKee, E. Minet, C. Stern, S. Riahi, C. D. Stiles, and P. a Silver, "A genome-wide in situ hybridization map of RNA-binding proteins reveals anatomically restricted expression in the developing mouse brain.," *BMC Dev. Biol.*, vol. 5, p. 14, 2005.

[15] M. N. Hinman, H. L. Zhou, A. Sharma, and H. Lou, "All three RNA recognition motifs and the hinge region of HuC play distinct roles in the regulation of alternative splicing," *Nucleic Acids Res.*, vol. 41, no. 9, pp. 5049–5061, 2013.

[16] K. W. Yau, S. F. B. vanBeuningen, I. Cunha-Ferreira, B. M. C. Cloin, E. Y. vanBattum, L. Will, P. Schätzle, R. P. Tas, J. vanKrugten, E. a. Katrukha, K. Jiang, P. S. Wulf, M. Mikhaylova, M. Harterink, R. J. Pasterkamp, A. Akhmanova, L. C. Kapitein, and C. C. Hoogenraad, "Microtubule minus-end binding protein CAMSAP2 controls axon specification and dendrite development," *Neuron*, vol. 82, no. 5, pp. 1058–1073, 2014.

[17] M. a M. Franker and C. C. Hoogenraad, "Microtubule-based transport - basic mechanisms, traffic rules and role in neurological pathogenesis.," *J. Cell Sci.*, vol. 126, no. Pt 11, pp. 2319–29, 2013.

[18] Y. Noda, R. Sato-Yoshitake, S. Kondo, M. Nangaku, and N. Hirokawa, "KIF2 is a new microtubule-based anterograde motor that transports membranous organelles distinct from those carried by kinesin heavy chain or KIF3A/B," *J. Cell Biol.*, vol. 129, no. 1, pp. 157–167, 1995.

[19] L. E. Simone and J. D. Keene, “Mechanisms coordinating ELAV/Hu mRNA regulons,” *Curr. Opin. Genet. Dev.*, vol. 23, no. 1, pp. 35–43, 2013.

[20] J. Dalmau, H. M. Furneaux, C. Cordon-Cardo, and J. B. Posner, “The expression of the Hu (paraneoplastic encephalomyelitis/sensory neuronopathy) antigen in human normal and tumor tissues.,” *Am. J. Pathol.*, vol. 141, no. 4, pp. 881–886, 1992.

[21] A. C. Beckel-Mitchener, A. Miera, R. Keller, and N. I. Perrone-Bizzozero, “Poly(A) tail length-dependent stabilization of GAP-43 mRNA by the RNA-binding protein HuD,” *J. Biol. Chem.*, vol. 277, no. 31, pp. 27996–28002, 2002.

[22] X. Wang and T. M. Tanaka Hall, “Structural basis for recognition of AU-rich element RNA by the HuD protein.,” *Nat. Struct. Biol.*, vol. 8, no. 2, pp. 141–145, 2001.

[23] W. Akamatsu, H. Fujihara, T. Mitsuhashi, M. Yano, S. Shibata, Y. Hayakawa, H. J. Okano, S.-I. Sakakibara, H. Takano, T. Takano, T. Takahashi, T. Noda, and H. Okano, “The RNA-binding protein HuD regulates neuronal cell identity and maturation.,” *Proc. Natl. Acad. Sci. U. S. A.*, vol. 102, no. 12, pp. 4625–4630, 2005.

[24] M. Mazumdar, M.-H. Sung, and T. Misteli, “Chromatin maintenance by a molecular motor protein,” *Nucleus*, vol. 2, no. 6, pp. 591–600, 2011.

[25] N. Hirokawa, Y. Noda, Y. Tanaka, and S. Niwa, “Kinesin superfamily motor proteins and intracellular transport,” *Nat Rev Mol Cell Biol*, vol. 10, no. 10, pp. 682–696, Oct. 2009.

[26] N. Hirokawa, S. Niwa, and Y. Tanaka, “Molecular motors in neurons: Transport mechanisms and roles in brain function, development, and disease,” *Neuron*, vol. 68, no. 4, pp. 610–638, 2010.

[27] H. Aizawa, Y. Sekine, R. Takemura, Z. Zhang, M. Nangaku, and N. Hirokawa, “Kinesin family in murine central nervous system,” *J. Cell Biol.*, vol. 119, no. 5, pp. 1287–1296, 1992.

[28] D. H. Hall and E. M. Hedgecock, “Kinesin-related gene unc-104 is required for axonal transport of synaptic vesicles in C. elegans,” *Cell*, vol. 65, no. 5, pp. 837–847, May 1991.

[29] H. Miki, M. Setou, K. Kaneshiro, and N. Hirokawa, “All kinesin superfamily protein, KIF, genes in mouse and human.,” *Proc. Natl. Acad. Sci. U. S. A.*, vol. 98, no. 13, pp. 7004–7011, 2001.

[30] N. Hirokawa, “Intracellular Transport and Kinesin Superfamily Proteins : Structure Dynamics and Function,” *Nat. Cell Biol.*, vol. 7, no. 2005, pp. 2006–2006, 2006.

[31] S. Niwa, K. Nakajima, H. Miki, Y. Minato, D. Wang, and N. Hirokawa, “KIF19A Is a Microtubule-Depolymerizing Kinesin for Ciliary Length Control,” *Dev. Cell*, vol. 23, no. 6, pp. 1167–1175, 2012.

[32] L. Cheng, J. Desai, C. J. Miranda, J. S. Duncan, W. Qiu, A. a. Nugent, A. L. Kolpak, C. C. Wu, E. Drokhlyansky, M. M. Delisle, W. M. Chan, Y. Wei, F. Propst, L. R. P. Samara, B. Fritzsch, and E. C. Engle, “Human CFEOM1 mutations attenuate KIF21A autoinhibition and cause oculomotor axon stalling,” *Neuron*, vol. 82, no. 2, pp. 334–349, 2014.

[33] K. Yamada, C. Andrews, W.-M. Chan, C. a McKeown, A. Magli, T. de Berardinis, A. Loewenstein, M. Lazar, M. O’Keefe, R. Letson, A. London, M. Ruttum, N. Matsumoto, N. Saito, L. Morris, M. Del Monte, R. H. Johnson, E. Uyama, W. a Houtman, B. de Vries, T. J. Carlow, B. L. Hart, N. Krawiecki, J. Shoffner, M. C. Vogel, J. Katowitz, S. M. Goldstein, A. V Levin, E. C. Sener, B. T. Ozturk, a N. Akarsu, M. C. Brodsky, F. Hanisch, R. P. Cruse, A. a Zubcov, R. M. Robb, P. Roggenkäemper, I. Gottlob, L. Kowal, R. Battu, E. I. Traboulsi, P. Franceschini, A. Newlin, J. L. Demer, and E. C. Engle, “Heterozygous mutations of the kinesin KIF21A in congenital fibrosis of the extraocular muscles type 1 (CFEOM1).,” *Nat. Genet.*, vol. 35, no. 4, pp. 318–321, 2003.

[34] C. Y. Jang, J. Wong, J. a. Coppinger, A. Seki, J. R. Yates, and G. Fang, “DDA3 recruits microtubule depolymerase Kif2a to spindle poles and controls spindle dynamics and mitotic chromosome movement,” *J. Cell Biol.*, vol. 181, no. 2, pp. 255–267, 2008.

[35] L. Wordeman, “Microtubule-depolymerizing kinesins,” *Curr. Opin. Cell Biol.*, vol. 17, no. 1, pp. 82–88, 2005.

[36] C.-Y. Jang, J. a Coppinger, A. Seki, J. R. Yates, and G. Fang, “Plk1 and Aurora A regulate the depolymerase activity and the cellular localization of Kif2a.,” *J. Cell Sci.*, vol. 122, no. Pt 9, pp. 1334–1341, 2009.

[37] L. a. Cameron, G. Yang, D. Cimini, J. C. Canman, O. Kisurina-Evgenieva, A. Khodjakov, G. Danuser, and E. D. Salmon, “Kinesin 5-independent poleward flux of kinetochore microtubules in PtK1 cells,” *J. Cell Biol.*, vol. 173, no. 2, pp. 173–179, 2006.

[38] Y. Noda, S. Niwa, N. Homma, H. Fukuda, S. Imajo-Ohmi, and N. Hirokawa, “Phosphatidylinositol 4-phosphate 5-kinase alpha (PIPK) regulates neuronal microtubule depolymerase kinesin, KIF2A and suppresses elongation of axon branches,” *Proc. Natl. Acad. Sci.*, vol. 109, no. 5, pp. 1725–1730, 2012.

[39] A. Desai, S. Verma, T. J. Mitchison, and C. E. Walczak, “Kin I kinesins are microtubule-destabilizing enzymes,” *Cell*, vol. 96, no. 1, pp. 69–78, 1999.

[40] V. S. Caviness, T. Takahashi, and R. S. Nowakowski, “Numbers, time and neocortical neuronogenesis: a general developmental and evolutionary model.,” *Trends Neurosci.*, vol. 18, no. 9, pp. 379–383, 1995.

[41] P. Rakic and V. S. Caviness, “Cortical development: view from neurological mutants two decades later.,” *Neuron*, vol. 14, no. 6, pp. 1101–1104, 1995.

[42] a. J. Barkovich, R. Guerrini, R. I. Kuzniecky, G. D. Jackson, and W. B. Dobyns, “A developmental and genetic classification for malformations of cortical development: Update 2012,” *Brain*, vol. 135, no. 5, pp. 1348–1369, 2012.

[43] S. L. Rogers and V. I. Gelfand, “Membrane trafficking, organelle transport, and the cytoskeleton,” *Curr. Opin. Cell Biol.*, vol. 12, no. 1, pp. 57–62, 2000.

[44] K. J. Roux, D. I. Kim, M. Raida, and B. Burke, “A promiscuous biotin ligase fusion protein identifies proximal and interacting proteins in mammalian cells,” *J. Cell Biol.*, vol. 196, no. 6, pp. 801–810, 2012.

[45] B. Westermann, “Mitochondrial fusion and fission in cell life and death.,” *Nat. Rev. Mol. Cell Biol.*, vol. 11, no. 12, pp. 872–884, 2010.

VITA

Cansu Akkaya was born on 17.10.1991, in Izmir, Turkey. She received her major B.Sc degree in Molecular Biology and Genetics from Middle East Technical University (METU), Ankara in 2013. From September 2013 to August 2015 she worked as both teaching and research assistant at Koç University. She worked on “Effects of KIF2A protein isoforms and *Kif2a* disease mutations on neuronal function” during her M.Sc studies.

Appendix A: Cloning of *Elavl2, Elavl3 and Elavl4* into pcDNA4A backbone vector

Total RNA Isolation

Cortices from mice at postnatal day 21 were collected for total RNA isolation. 1ml of Qiazol (Qiagen, Cat. #79306) was added per 100 mg of tissue. Tissues were dissociated by pipetting and incubated for 5 minutes at room temperature. 200 µl of chloroform was added per 1ml of homogenate and homogenates were shaken vigorously for 15 seconds and incubated for 3 minutes at room temperature. Homogenates were centrifuged at 14000xg for 15 minutes at 4^{o}C. Upper aqueous phase was transferred into new 1.5 ml centrifuge tubes. 500 µl of isopropanol was added per 1ml of homogenate and mixed by vortexing and left at room temperature for 10 minutes. Samples were centrifuged at 14000xg for 10 minutes at 4^{o}C. Supernatant was removed and at this stage RNA pellet was visible at the bottom of tubes. Pellet was washed with 1ml of RNase free 75% ethanol. Samples were centrifuged at 10000xg for 5 minutes at 4^{o}C. Supernatant was removed and pellet was air dried under tissue culture hood. RNA pellet was dissolved in 50 µl of nuclease free ddH_2O.

cDNA synthesis and cloning

cDNA was synthesized using Standard Procedure for Qualitative RT-PCR of Transcriptor High Fidelity cDNA synthesis Kit (Roche, Cat. #05091284001) from 100 ng total RNA (postnatal 21 day cortex). Briefly, 100 ng/µl of total RNA was mixed with 60µM random hexamer primer. Template primer mixture was denatured by heating tube at 65^{o}C for 10 minutes. After incubation, 1X Transcriptor High Fidelity Reverse Transcriptase Reaction buffer, 20 Unit RNase inhibitor, 1mM deoxynucleotide mix, 5mM DTT and 10 Unit Transcriptor High Fidelity Reverse Transcriptase (RTase) was added into tube and incubated at 50^{o}C for 30 minutes and 85^{o}C for 5 minutes. Negative control of this reaction is the tube that does not contain RTase.

PCR was set up in 30 µl reaction mixture containing 1X Phusion HF reaction buffer, 300µM dNTP's, 0.5µM forward and 0.5µM reverse primers (Appendix C), 1 µl template DNA and 1 Unit Phusion Hot Start Flex DNA Polymerase. Conditions of PCR for denaturing, annealing and extension were set to 98^{o}C for 15 seconds, 56^{o}C for 30 seconds, and 72^{o}C for 1.5 minutes respectively and the cycle number was 40. PCR products were run on agarose gel and the correct band was excised under UV light and DNA extraction from agarose gel was performed using EZ-10 Spin column DNA Gel Extraction Kit. Forward primer that used in PCR contained BamHI (for *Elavl2* and *Elavl3*) and HindIII (for *Elavl4*) restriction enzyme cut site and reverse primer contained EcoRI (for *Elavl2* and *Elavl3*) and XhoI (for *Elavl4*) restriction enzyme site. Restriction enzyme digestion was set up in 20 µl reaction mixture containing 2X Tango Buffer (Thermo Scientific, Cat. #BY5) for *Elavl2* and *Elavl3* and 1X Buffer R (Thermo Scientific, Cat. #BR5) for *Elavl4*, 5 Unit BamHI (Thermo Scientific, Cat. #ER0051) and 5 Unit EcoRI (Thermo Scientific, Cat. #ER0271) for *Elavl2* and *Elavl3* and 5 Unit HindIII (Thermo Scientific, Cat. #ER0501) and 5 Unit XhoI (Thermo Scientific, Cat. #ER0691) for *Elavl4* and 10 µl agarose extracted DNA or pcDNA4A 0.5 µl plasmid. Samples were double-digested at 37^{o}C overnight. Next day, 1 µl of FastAP (Alkaline phosphatase) added to reaction mix to prevent self-ligation. Both PCR products and backbone plasmid DNA were purified with PCR purification kit. 50 ng pcDNA4A vector was ligated with digested PCR products in a 10 µl reaction mixture containing, 1X T4 Ligase Buffer, 5 Unit T4 ligase and incubated at room temperature for 2 hours.

1 µl of ligation product was transformed into chemically competent DH5α *E.coli* cells by using heat shock method. Cells were plated on LB/ampicillin plates. Miniprep cultures were incubated at 37^{o}C overnight with constant shaking and plasmid DNA's were purified by GeneJET Plasmid Miniprep Kit. Diagnostic digestion was set up in 20 µl reaction mixture containing 1µl of DNA, 2X Tango Buffer for *Elavl2* and *Elavl3* and 1X

Buffer R for Elavl4, 5 Unit BamHI and 5 Unit EcoRI for *Elavl2* and *Elavl3* and 5 Unit HindIII and 5 Unit XhoI for *Elavl4.* Samples were double digested at 37^{o}C for 2 hours and run on agarose gel to confirm that selected colonies had correct size insert. Concentrations were measured by using NanoDrop2000c and 5 µl of miniprep DNA's were sent to direct sequencing for validation. After confirming that miniprep DNA's had correct insertions, maxi-prep cultures were incubated at 37^{o}C overnight with constant shaking and plasmid DNA's that contained *Elavl2* was purified with Endofree® Plasmid Maxi Kit, *Elavl3* and *Elavl4* were purified with GeneJet Plasmid Maxiprep Kit (Thermo Scientific, Cat.#K0491).

Appendix B: Determination of nELAVL regulation of *Kif2a* mRNA at Different Developmental Time Points

Lysate preparation from mouse cortex tissue

Cortices from mice at different time points (embryonic day 14, 16, 18, postnatal day 0, 7, 14, 21, 28 and adult) were dissected in ice-cold 1X PBS. Cortices were put into homogenizer and tissues were homogenized in 500 µl of cold 1X PBS. Homogenized tissues were transferred into 1.5 ml centrifuge tubes and samples were spin down for 10 seconds. 100 µl of 1X RIPA Buffer (10X RIPA: 0.05M Tris-HCl pH7.5, 0.15M NaCl, 1% Triton X-100, 1%Na-DOC, 0.1% SDS; glycerol, 1X 2M NEM, 1X protease inhibitor and 1X phosphatase inhibitor (Thermo Scientific, Cat. #78420)) per 0.1g of homogenate was added onto samples and samples were dissolved by pipetting. Sonication was done for 7 seconds, 10 cycles at cold room. Samples were centrifuged at 14000 rpm for 10 minutes at 4^{o}C and supernatant was transferred into fresh 1.5 ml centrifuge tubes and stored at -20^{o}C for western blotting.

cDNA synthesis

Cortices from mice at different time points (embryonic day 14, 16, 18, postnatal day 0, 7, 14, 21, 28 and adult) were dissected in ice-cold 1X PBS for RNA isolation. RNA was isolated by using the RNA isolation procedure which was explained in Appendix A.

cDNA was synthesized using Standard Procedure for Quantitative RT-PCR of Transcriptor High Fidelity cDNA synthesis Kit from 250ng total RNA. Briefly, 500 ng/µl of total RNA was mixed with 60 µM random hexamer primer. Template primer mixture was denatured by heating tube at 65^{o}C for 10 minutes. After incubation, 1X Transcriptor High Fidelity Reverse Transcriptase Reaction buffer, 20 Unit RNase inhibitor, 1mM deoxynucleotide mix, 5 mM DTT and 10 Unit Transcriptor High Fidelity Reverse Transcriptase (RTase) was added into tube and incubated at 29^{o}C for 10 minutes, 48^{o}C for 60 minutes and 85^{o}C for 5 minutes and the cover temperature was 50^{o}C. Negative control of this reaction is the tube that does not contain RTase.

Real Time PCR (Q-PCR)

To determine the primer efficiency designed for KIF2A.1 and KIF2A.2 quantitative Real Time PCR was performed using Luminaris HiGreen qPCR Master Mix (Thermo scientific, Cat. #K0991). Briefly, 1X Master Mix, 0.3 µM forward primer, 0.3 µM reverse primer and 500 ng template cDNA was mixed and incubated at 95^{o}C for 10 seconds, 60^{o}C for 20 seconds and 72^{o}C for 20 seconds for 35 cycles. After that, Q-PCR was done to find the amount of different KIF2A isoforms at different developmental times (E14, E16, E18, P0, P7, P14, P21, P28 and adult). This time 2500 pg of cDNA was used and QPCR conditions for denaturing, annealing and extension steps were 95^{o}C for 10 seconds, 61^{o}C for 20 seconds and 72^{o}C for 20 seconds, respectively for 35 cycles.

Primer efficiencies were calculated by the following formula:

(10^(-1/m)-1)*100 where; y=mx+b

y: Ct value (cycle #)

x: log of concentration

m: slope of the graph

b: y-intercept

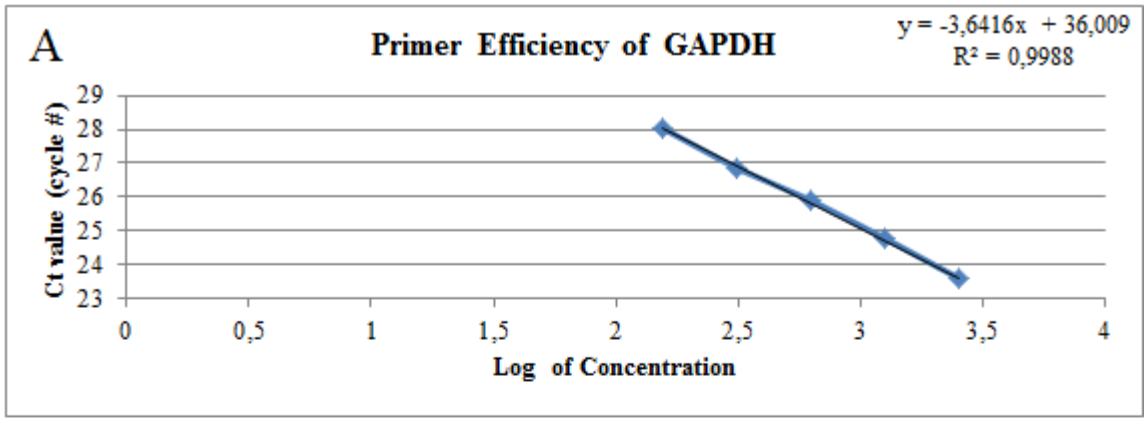
A
Primer Efficiency of GAPDH
y = -3,6416x + 36,009
R² = 0,9988
Ct value (cycle #)
29
28
27
26
25
24
23
0
0,5
1
1,5
2
2,5
3
3,5
4
Log of Concentration

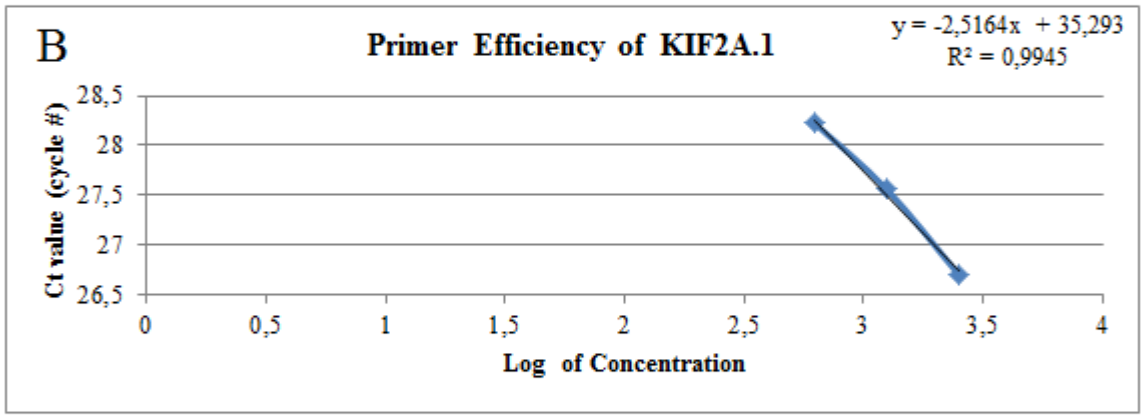
B
Primer Efficiency of KIF2A.1
y = -2,5164x + 35,293
R² = 0,9945
Ct value (cycle #)
28,5
28
27,5
27
26,5
0
0,5
1
1,5
2
2,5
3
3,5
4
Log of Concentration

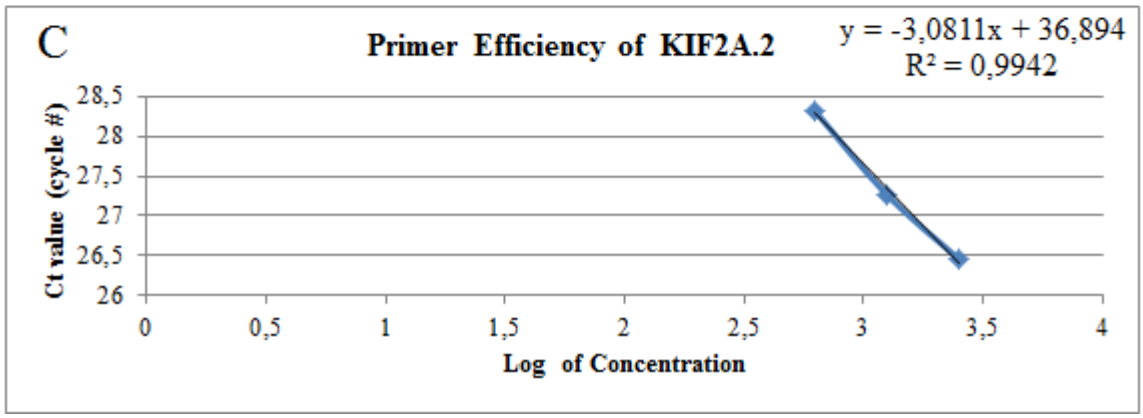
C
Primer Efficiency of KIF2A.2
y = -3,0811x + 36,894
R² = 0,9942
Ct value (cycle #)
28,5
28
27,5
27
26,5
26
0
0,5
1
1,5
2
2,5
3
3,5
4
Log of Concentration

Figure A.1: Primer efficiencies of KIF2A.1 and KIF2A.2 were determined by using Luminaris HiGreen qPCR master mix. cDNA concentrations were 2500 pg, 1250 pg, and 625 pg reactions were set up in duplicates for each primer. Two negative controls were used: no RTase was used as one negative control and in the second negative control water was added instead of cDNA. **A.** Efficiency of primer designed against GAPDH is 88%. **B.** Efficiency of primer designed against KIF2A.1 is 100%. **C.** Efficiency of primer designed against KIF2A.2 is 100%.

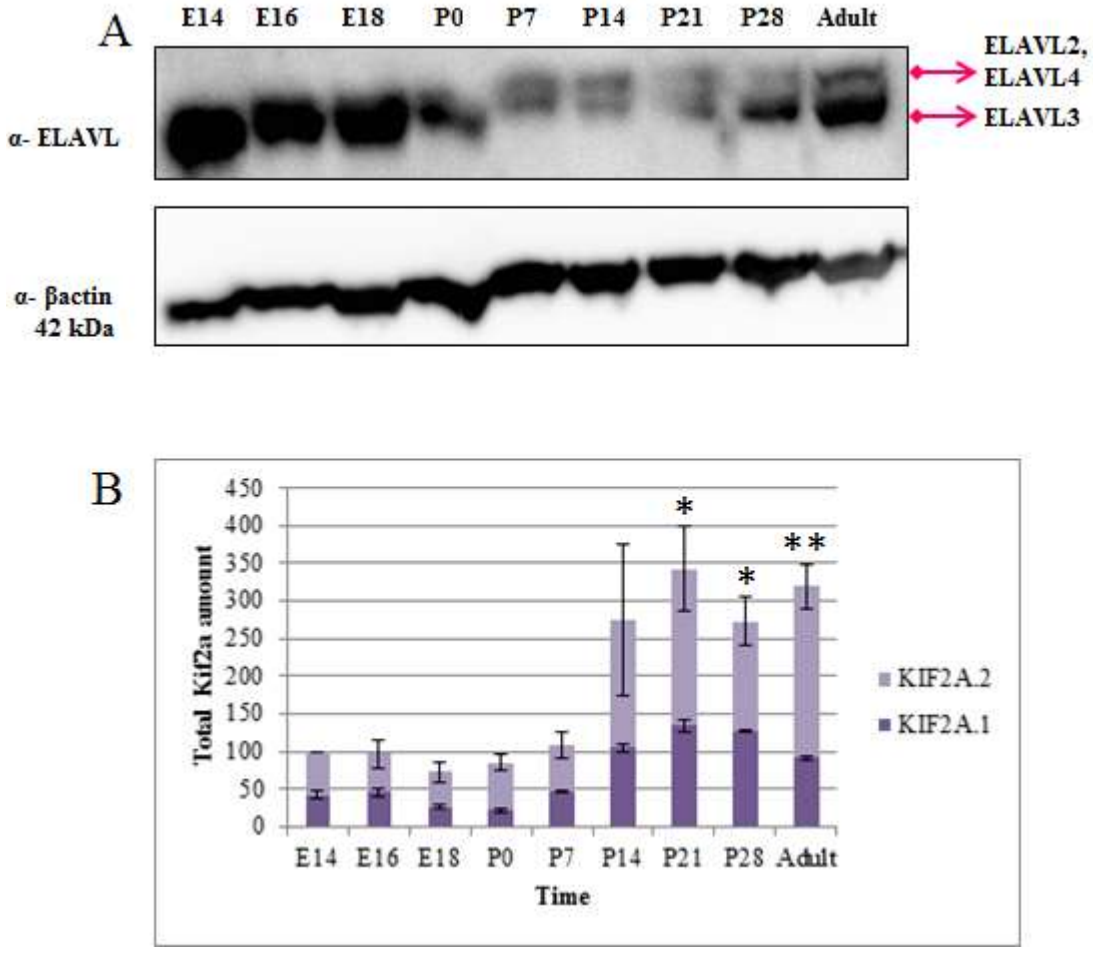

Figure A.2: nELAVL protein expression is developmentally controlled. **A.** Western blot against endogenous nELAVL showed that nELAVL expression decreased at P0 stage. Upper band represents ELAVL2 and ELAVL4, lower band represents both ELAVL3. β-actin is the loading control. **B.** Relative KIF2A isoforms' mRNA expression (normalized to E14) quantified by Q-PCR analysis. P21 and the upper stages total KIF2A mRNA amount increased and it was highest in adult stage. Error bar indicates the standard error and *$p<0.02$, **$p<0.005$

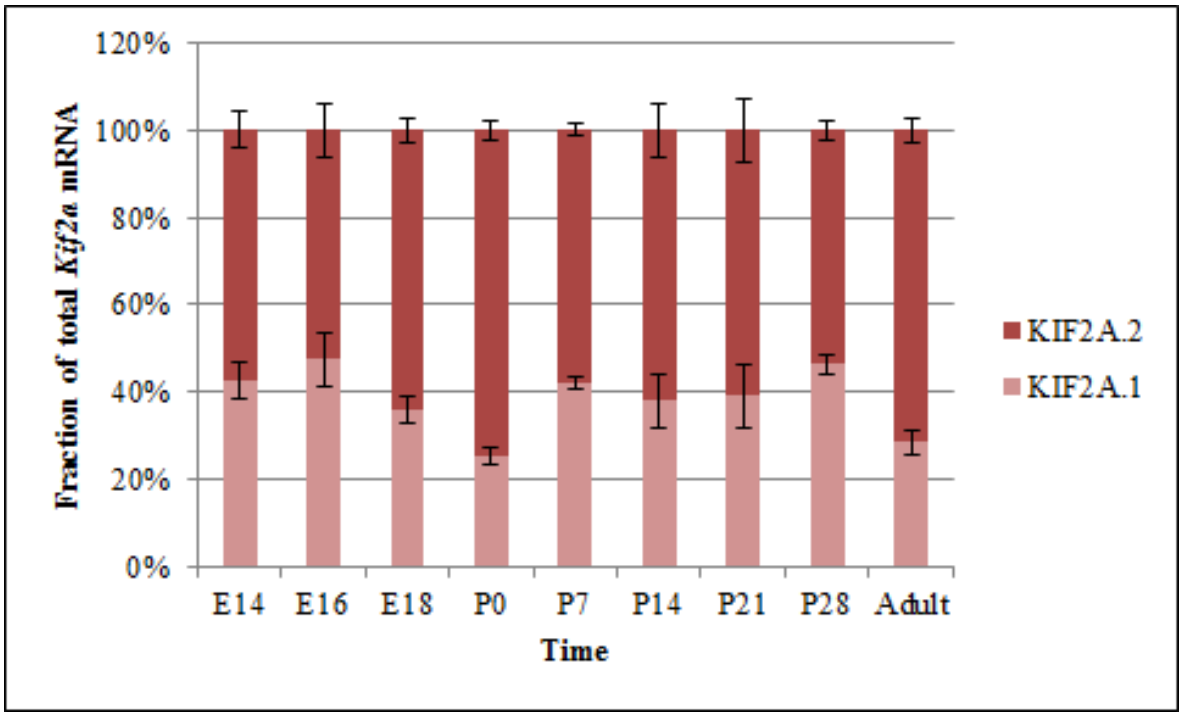

Figure A.3: *Kif2a* exon18 alternative splicing does not change during development.

Q-PCR were done by using *Kif2a.1* and *Kif2a.2* specific primers and result showed that there is no significant difference between *Kif2a.1* and *Kif2a.2* mRNA compositions at different developmental time points. Error bar indicates the standard error.

Appendix C: Primer List

Primer Name	Primer Sequence
Kif2a_BirA_N_XhoI_F	5’-AAACTCGAGATGGTAACATCTTTAAATGAAGAT-3’
Kif2a_BirA_N_EcoRI_R	5’-AAAGAATTCTTAGAGGGCTCGGGGCCTCTTGGG-3’
Kif2a_c959G>A_F	5’-GCAGACTGGAAATGGGAAAACTCATACTATGG-3’
Kif2a_c961C>G_F	5’-GCAGACTGGAAGTGGGAAAACTGATACTATGG-3’
Kif2a_sdm_R	5’-CCATAAGCAAAGCACGTAGCCATGCCCCTTT-3’
GAPDH_QPCR_F3	5’-CGACTTCAACAGCAACTCCCATCTTCC-3’
GAPDH_QPCR_R3	5’-TGGGTGGTCCAGGGTTTCTTACTCCTT-3’
Kif2a-KIF2A.1-F	5’-CCAGGGTGAAAGAATTGACTG-3’
Kif2a- KIF2A.1-R	5’-GCTTCATGGAAAGTGAACAGC-3’
Kif2a- KIF2A.2-F	5’-GCAAATAGGGTGAAAGAATTGACT-3’
Kif2a- KIF2A.2- R	5’-TCTGGGAGACAGCTTCATGG-3’
Elavl2-BamHI-F	5’-AAAGGATCCATGGAAACACAACTGTCTAATTGGG-3’
Elavl2-EcoRI-R	5’-AAAGAATTCGGCTTTGTGCGTTTTGTTTGTCTT-3’
Elavl3-BamHI-F	5’-AAAGGATCCATGGTCACTCAGATACTGGGGGCC-3’
Elavl3-EcoRI-R	5’-AAAGAATTCGGCCTTGTGCTGCTTGCTGGTCTTG-3’
Elavl4_HindIII_Fv2	5’-AAAAAGCTTATGGTTATGATAATTAGCACCATG-3’
Elavl4_XhoI_R	5’-AAACTCGAGGGATTTGTGGGCTTTGTTGGT-3’